Plastidial Thioredoxin *z* Interacts with Two Fructokinase-Like Proteins in a Thiol-Dependent Manner: Evidence for an Essential Role in Chloroplast Development in *Arabidopsis* and *Nicotiana benthamiana* [C][W]

Borjana Arsova,[a,1] Ursula Hoja,[b,1] Matthias Wimmelbacher,[b,1] Eva Greiner,[b] Şuayib Üstün,[b] Michael Melzer,[c] Kerstin Petersen,[a] Wolfgang Lein,[a] and Frederik Börnke[b,2]

[a] Max-Planck Institute of Molecular Plant Physiology, 14476 Golm, Germany
[b] Department Biologie, Lehrstuhl für Biochemie, Friedrich Alexander Universität Erlangen-Nürnberg, 91058 Erlangen, Germany
[c] Leibniz Institute of Plant Genetics and Crop Plant Research, 06466 Gatersleben, Germany

Here, we characterize a plastidial thioredoxin (TRX) isoform from *Arabidopsis thaliana* that defines a previously unknown branch of plastidial TRXs lying between *x*- and *y*-type TRXs and thus was named TRX *z*. An *Arabidopsis* knockout mutant of TRX *z* had a severe albino phenotype and was inhibited in chloroplast development. Quantitative real-time RT-PCR analysis of the mutant suggested that the expressions of genes that depend on a plastid-encoded RNA polymerase (PEP) were specifically decreased. Similar results were obtained upon virus-induced gene silencing (VIGS) of the *TRX z* ortholog in *Nicotiana benthamiana*. We found that two fructokinase-like proteins (FLN1 and FLN2), members of the pfkB-carbohydrate kinase family, were potential TRX *z* target proteins and identified conserved Cys residues mediating the FLN–TRX z interaction. VIGS in *N. benthamiana* and inducible RNA interference in *Arabidopsis* of FLNs also led to a repression of PEP-dependent gene transcription. Remarkably, recombinant FLNs displayed no detectable sugar-phosphorylating activity, and amino acid substitutions within the predicted active site imply that the FLNs have acquired a new function, which might be regulatory rather than metabolic. We were able to show that the FLN2 redox state changes in vivo during light/dark transitions and that this change is mediated by TRX *z*. Taken together, our data strongly suggest an important role for TRX *z* and both FLNs in the regulation of PEP-dependent transcription in chloroplasts.

INTRODUCTION

Thioredoxins (TRXs) are small (~12 to 14 kD) heat-stable thiol:disulphide oxidoreductases critical for redox regulation of protein function in all free-living organisms (Buchanan and Balmer, 2005). Each TRX contains a redox-active disulfide bridge in its active site with a conserved amino acid sequence CXXC (where X indicates variable residues). In the reduced state, TRXs are able to reduce disulfide bridges in numerous target proteins. Initially described as hydrogen carriers in ribonucleotide reduction in *Escherichia coli*, they have also been found to function in defense against oxidative stress by providing reducing power to thiol-containing antioxidant proteins. Alternatively, TRXs can directly modulate the activity of a given target protein by reduc-

tion of a disulfide bond (Buchanan and Balmer, 2005; Gelhaye et al., 2005).
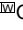
Plants are distinguishable from other organisms by their very complex TRX system. A recent inspection of the *Arabidopsis thaliana* genome revealed the presence of at least 20 TRX genes and more than 40 additional TRX-like genes encoding proteins for which there are no biochemical data available but which possess significant similarity to TRXs (Meyer et al., 2005, 2008). *Arabidopsis* TRXs belong to six major groups, *f*, *m*, *h*, *o*, *x*, and *y*, that are located in various subcellular compartments, including the chloroplast, mitochondria, and cytosol. Depending on their subcellular localization, TRXs are reduced by a different electron donor system. Both cytosolic and mitochondrial TRXs are reduced with electrons from NADPH via compartment-specific NADPH/TRX reductases (NTRs), whereas the chloroplast TRXs are reduced by the ferredoxin/TRX reductase with electrons provided by photosynthetic electron transport (Schürmann and Jacquot, 2000). In addition, chloroplasts contain a modified type of NTR, designated NTRC, which harbors a TRX domain in a C-terminal extension (Serrato et al., 2004). NTRC is able to conjugate NTR and TRX activities to efficiently reduce 2-Cys peroxiredoxin using NADPH as a source of reducing power (Spinola et al., 2008) and was further shown to be involved in the redox regulation of ADP-glucose pyrophosphorylase, a central enzyme of starch synthesis (Michalska et al., 2009).

The largest TRX group in *Arabidopsis* consists of eight *h*-type TRXs that are generally thought to be cytosolic proteins, although TRX *h2* has been shown to locate to mitochondria (Gelhaye et al., 2004). The *o*-type TRXs possess a predicted N-terminal mitochondrial target peptide, and mitochondrial import assays have confirmed this localization (Laloi et al., 2001).

The chloroplast TRX system is particularly complex. Type *m* and *f* TRXs were initially identified as the light-dependent regulators of key enzymes of photosynthetic metabolism in chloroplasts: TRX *f* preferentially activates fructose-1,6-bisphosphatase and TRX *m* preferentially activates NADP-malate dehydrogenase (Buchanan, 1980). Four *m*-type and two *f*-type TRXs have been identified in *Arabidopsis*. Whereas the latter have mainly been implicated in redox regulation of photosynthetic carbon assimilation, *m*-type TRXs might also play additional roles (Issakidis-Bourguet et al., 2001; Meyer et al., 2005). Type *x* and *y* TRXs are represented by one and two genes, respectively, in the *Arabidopsis* genome, and based on their ability to reduce 2-Cys peroxiredoxins, these TRXs appear to be involved in protecting the plastid against oxidative damage (Collin et al., 2003, 2004).

The diversity of plant TRXs implies that numerous TRX target proteins might exist and raises the question about functional specificity or redundancy of particular TRX isoforms. Recent proteomic studies, such as thioredoxin-trapping chromatography or labeled gel electrophoresis, both in combination with protein identification by mass spectrometry, have identified >180 potential TRX target proteins in plants (Motohashi et al., 2001; Balmer et al., 2003, 2004b, 2006; Wong et al., 2004; Marchand et al., 2006; Alkhalfioui et al., 2007). However, the vast majority of these have yet not been experimentally verified, and in vitro methods appear to suffer from an inherent lack of specificity as chloroplast targets have been identified with cytosolic TRX as bait and vice versa (Meyer et al., 2008). Genetic approaches to define isoform-specific functions for individual TRXs in *Arabidopsis* knockout plants have largely been limited by the absence of phenotypes in single mutants, presumably due to functional redundancy within gene families (Meyer et al., 2008). Recently, it has been shown that RNA interference–mediated downregulation of a *TRX m* isoform in transgenic rice (*Oryza sativa*) plants resulted in phenotypic alterations, including leaf chlorosis and abnormal chloroplast structure (Chi et al., 2008). In these plants, 2-Cys peroxiredoxin was present in its oxidized form and H_2O_2 levels were increased, suggesting that TRX *m* in rice is directly or indirectly involved in the protection against oxidative stress (Chi et al., 2008).

To shed further light on TRX function in plants, we searched the *Arabidopsis* genome for previously uncharacterized TRX isoforms. In this study, we have characterized a plastidic TRX isoform that, based on its phylogenetic relationship to other plastidial TRXs, was named TRX *z*. Loss-of-function analyses in *Arabidopsis* and *Nicotiana benthamiana* indicate that TRX is essential for proper chloroplast development, most likely through regulating plastid-encoded polymerase (PEP) dependent chloroplast transcription. Furthermore, we show that TRX *z* interacts with two fructokinase-like proteins (FLNs), both of which appear to be necessary for PEP-dependent gene expression in chloroplasts. Based on our results, we speculate that TRX *z* and the two FLNs define a heretofore unknown protein interaction module essential for chloroplast development.

RESULTS

Arabidopsis Gene At3g06730 Defines a Previously Unrecognized Group of Chloroplast Thioredoxins

To identify previously uncharacterized TRXs encoded by the *Arabidopsis* genome, we used BLASTP to search the *Arabidopsis* protein set lodged with The Arabidopsis Information Resource (TAIR; www.Arabidopsis.org). When using TRX *x* as query sequence, a BLASTP hit (At3g06730) with low, albeit significant, similarity (E-value 1.0 e^{-11}) to TRX *x* could be identified. The protein, annotated as thioredoxin family protein, contains the characteristic TRX active site signature $C_{106}GPC_{109}$ (redox active Cys residues numbered according to their position in the polypeptide chain). In silico analysis of At3g06730 by ChloroP (Emanuelsson et al., 1999) strongly suggested that the protein contains a plastid targeting sequence with a potential cleavage site at amino acid position 81. To investigate the localization of At3g06730 in vivo, a C-terminal fusion between the first 81 amino acid residues of the precursor sequence and the green fluorescent protein (GFP) was transiently expressed in leaves of *N. benthamiana* plants using *Agrobacterium tumefaciens* infiltration. Confocal laser scanning microscopy of infiltrated leaves revealed that GFP fluorescence was exclusively associated with chloroplasts, demonstrating the targeting of At3g06730 to these organelles (Figure 1A). In control leaves expressing free GFP, the distribution of green fluorescence was clearly extrachloroplastic (Figure 1A).

To determine whether the At3g06730 protein shows disulfide reductase activity, insulin reduction assays were performed (Holmgren, 1979). In the presence of DTT, thioredoxin reduces the intermolecular disulfide bonds between the insulin A and B chains. Precipitation of the insoluble B chain can be measured photometrically by an increase in the absorbance at 650 nm. The assay was performed with recombinant His-tagged At3g06730 lacking the predicted chloroplast targeting peptide. As shown in Figure 1B, recombinant His-tagged At3g06730 was able to accelerate the reduction of insulin in the presence of DTT, clearly demonstrating that At3g06730 possesses disulfide reductase activity in vitro. These results led us to conclude that *At3g06730* encodes a previously unrecognized plastid-targeted TRX.

A phylogenetic tree built from the alignment of At3g06730 to other plastidic and mitochondrial TRXs from *Arabidopsis* revealed that *At3g06730* encodes a TRX relatively distant from previously identified TRXs, defining a new branch most related to *x*- and *y*-type TRXs (Figure 1C). In accordance with the previous TRX nomenclature, we thus named it TRX *z*.

Further homology searches made it possible to identify TRX *z* orthologs in many other plant species, including both dicots and monocots. Alignment of the sequences revealed that all sequences possess a variable N-terminal extension likely corresponding to a chloroplast transit peptide (see Supplemental Figure 1 online). Interestingly, the tomato (*Solanum lycopersicum*) ortholog of TRX *z* has previously been identified as an interaction partner of the resistance protein Cf-9 and hence was named CITRX (for Cf9-9-interacting thioredoxin) (Rivas et al., 2004). However, the wide distribution of TRX *z* in plants suggests that this type of chloroplast TRX has a more general function beyond that in Cf9-mediated disease resistance.
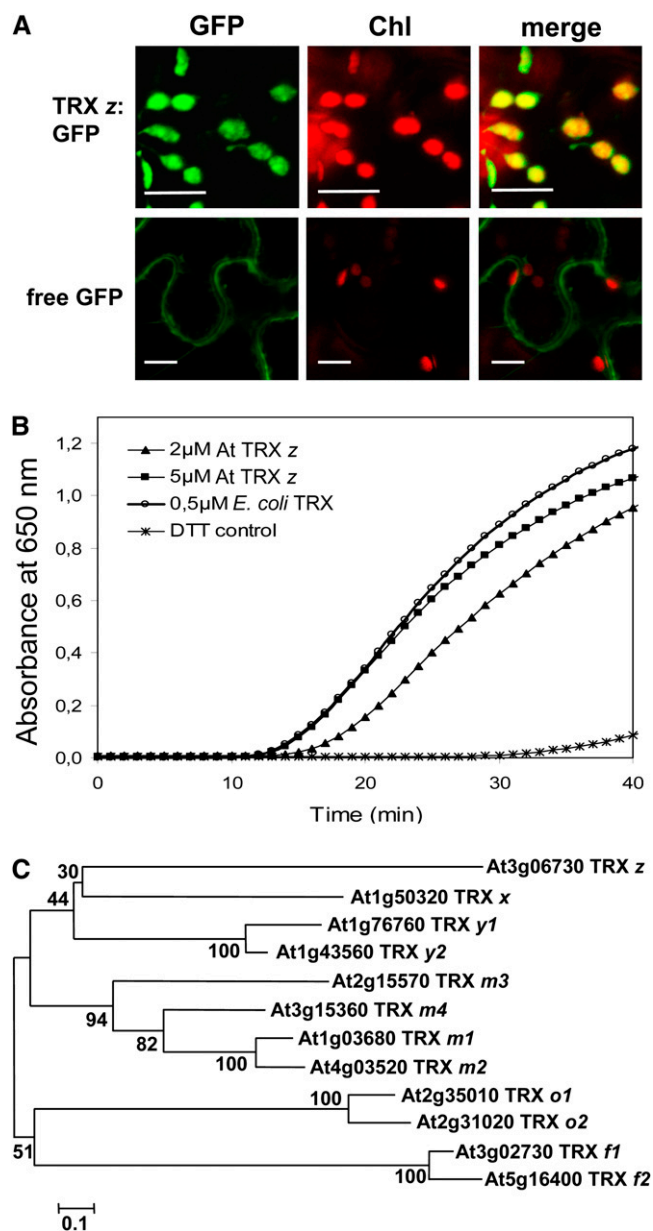
A

B

C

Figure 1. Characterization of At3g06730 as a Plastidial Thioredoxin.

(A) Subcellular localization of GFP alone (free GFP) or of a fusion between the first 81 amino acids of At3g06730 and GFP (TRX *z* TP: GFP) in tobacco leaves transiently transformed by *Agrobacterium* infiltration. The green fluorescence of GFP (left) and the red autofluorescence of chlorophyll (Chl, middle) were monitored separately using a confocal laser scanning microscope, and the two fluorescence images were merged (right). Bars = 10 μm.

(B) Measurement of disulfide reductase activity of recombinant His-tagged At3g06730 using the turbidimetric assay of insulin reduction. The incubation mixture contained 2 or 5 μM His-tagged At3g06730 protein lacking the predicted chloroplast targeting peptide. As a positive control, insulin reduction by 0.5 μM thioredoxin from *E. coli* was assayed. The nonenzymatic insulin reduction by DTT served as a negative control.

(C) Phylogenetic tree of plastidial and mitochondrial thioredoxins from *Arabidopsis*. At3g06730 occupies a position close to TRX *x* and *y* and

Loss of TRX *z* Function Strongly Affects Plant Phenotype

After having established that TRX *z* is a plastid-localized TRX, we next sought to investigate the role of TRX *z* in planta. An *Arabidopsis* T-DNA insertion line tagged in the first intron of the *TRX z* gene at position −428 of the genomic sequence relative to the start codon (Figure 2A) was identified from the SALK collection (Salk_028162C, *trx z*) and used for further analysis. A ratio of 161:62 kanamycin-resistant to -sensitive plants was observed when seeds of F2 plants were germinated on kanamycin. This is consistent with the 3:1 (72.2%:27.8%) ratio expected for a single T-DNA insert. Homozygous plants were obtained by self-pollination (Figure 2A). RT-PCR analysis showed that the *TRX z* transcript was absent in those plants, indicating a complete knockout (Figure 2A). Homozygous seedlings had pale yellowish leaves and were retarded in growth when grown on agar plates supplemented with sucrose (Figure 2B). When transferred to soil, seedlings ceased growth and subsequently died (data not shown). To prove further that the lack of *TRX z* transcript was responsible for phenotype of the homozygous *trx z* mutant, the full-length *TRX z* open reading frame driven by the 35S promoter was introduced into the *trx z* mutant background. As homozygous *trx z* plants are unable to grow autotrophically, transformation was performed in heterozygous plants. The phenotype of one representative homozygous BASTA-resistant T2 complemented line (out of six independent lines analyzed) is shown in Figure 2B. Complementation rescued the *trx z* mutant phenotype and restored growth on soil. Some leaves still displayed slight chlorosis at the leaf margins, suggesting that expression of the 35S promoter *TRX z* cDNA fusion did not yield complete rescue of the *trx z* mutant phenotype in specific cells. RT-PCR using primers specific for the *TRX z* coding region amplified a fragment in complemented plants but not in the untransformed *trx z* mutant (see Supplemental Figure 2 online). This result demonstrates that the expression of the *TRX z* open reading frame from the 35S promoter is sufficient to restore a green wild-type phenotype. Therefore, we conclude that *trx z* corresponds to a mutant allele of the *TRX z* gene and that TRX *z* is required for normal plant growth in *Arabidopsis*.

To gather additional evidence that TRX *z* is important for normal development in plants, we switched to transient virus-induced gene silencing (VIGS) in *N. benthamiana* and examined the biological function of the orthologous TRX isoform in this species. A database search identified an *N. benthamiana* sequence (see Supplemental Figure 1 online) that shared 98% similarity on the polypeptide level with TRX *z* from *Arabidopsis* throughout the predicted mature proteins. Thus, the protein was regarded as the *N. benthamiana* ortholog of *Arabidopsis* TRX *z* and subsequently named Nb-TRX *z* in our studies. A 120-bp

thus was named TRX *z*. The phylogenetic tree was constructed using MEGA 4 with the neighbor-joining method. Bootstrap values calculated from 1000 trials are shown at each node. The extent of divergence according to the scale (relative units) is indicated at the bottom. Predicted mature polypeptides lacking the putative transit peptide were employed for tree construction. The alignment used for this analysis is available as Supplemental Data Set 1 online.
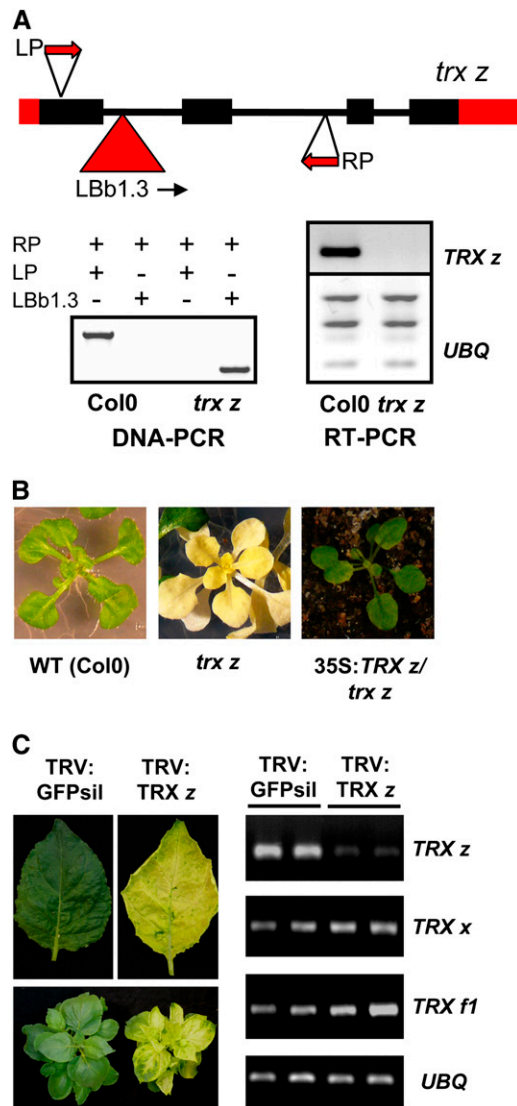
Figure 2. Characterization of *Arabidopsis* and *N. benthamiana* Plants with Reduced TRX *z* Expression.

(A) Molecular analysis of the *trx* z *Arabidopsis* T-DNA insertion mutant. The T-DNA insertion site and primer (LP, RP, and LB1.3) locations are indicated. PCR on genomic DNA revealed a homozygous insertion in the *TRX z* locus. Expression of *TRX z* transcript was shown by RT-PCR with gene-specific primer sets. Ubiquitin (*UBQ*) served as an internal control.
(B) Wild-type (WT; Col-0), *trx z*, and complemented (35S:*TRX z/trx z*) *Arabidopsis* plants. Three-week-old plants were grown on MS agar plates (Col-0 and *trx z*) or in soil (35S:*TRX z/trx z*), and their visible phenotype was observed.
(C) Chlorotic phenotype of TRV:TRX *z N. benthamiana* VIGS plants compared with control specimen (TRV:GFPsil). Photographs of leaves and whole plants were taken 14 d after inoculation (left). Transcript accumulation of *TRX z*, *TRX x*, and *TRX f1* in TRV:TRX *z* and control plants was analyzed by RT-PCR (right).

fragment from the variable 5′ end of the coding region predicted to specifically silence the Nb-TRX *z* isoform was cloned into a tobacco rattle virus (TRV) silencing vector (Liu et al., 2002b). Two weeks after silencing, the time used for all biological experiments in this work, TRV:TRX *z N. benthamiana* plants displayed severe leaf chlorosis in leaves that emerged after infiltration of the silencing constructs (Figure 2C). RT-PCR analysis showed decreased transcript levels for *TRX z*, confirming silencing of the target gene by TRV:TRX *z*, while the expression of two other TRX isoforms tested was not affected in TRV:TRX *z* plants (Figure 2C). The phenotype of the *TRX z*–silenced *N. benthamiana* plants closely resembled that of the *trx z Arabidopsis* knockout mutant, indicating that both proteins serve similar essential functions in these two plant species.

We used transmission electron microscopy to investigate morphological changes in the plastids of plants in which *TRX z* expression had been reduced or lost completely. As shown in Figure 3, plastids of *trx z* mutant *Arabidopsis* plants lacked internal membrane structures, such as stromal thylakoids or stacked grana thylakoids. In addition, there were many densely stained globular structures, probably plastoglobuli (Figure 3A). Organelle development in TRV:TRX *z N. benthamiana* plants is also severely impaired. Compared with the control plant, grana structures were unequally expanded and grana-interlacing stroma thylakoids are completely missing (Figure 3B).

Expression Analysis of Chloroplast-Encoded Genes

The chlorotic phenotype and the alterations in chloroplast ultrastructure of the *trx z Arabidopsis* knockout mutant and the TRV:TRX *z* VIGS plants suggests that TRX *z* is required for chloroplast biogenesis and differentiation. Recently, TRX *z* was identified by proteomics analysis as a component of plastid transcriptionally active chromosomes (TACs) isolated from mustard (*Sinapis alba*) and *Arabidopsis* (Pfalz et al., 2006). Plastid transcription depends on the plastid-encoded plastid RNA polymerase PEP and the nuclear-encoded plastid RNA polymerase NEP (Shiina et al., 2005). PEP preferentially transcribes photosynthesis-related genes in mature chloroplasts, whereas NEP preferentially transcribes housekeeping genes during early phases of development. Based on their promoter structures, plastid genes can be grouped into three classes (Hajdukiewicz et al., 1997). Transcription activities of many photosynthesis-related genes depend largely on PEP (class I), whereas genes from the *rpoB* operon and *accD* are transcribed exclusively by NEP (class III). Nonphotosynthetic housekeeping genes are generally transcribed by both PEP and NEP (class II).

If TRX *z* was related to one of the plastidial RNA polymerases, we anticipated specific transcriptional changes in chloroplast gene expression to occur in *trx z Arabidopsis* and TRV:TRX *z N. benthamiana* plants. Therefore, we used quantitative real-time RT-PCR to analyze the levels of transcripts that encode several chloroplast proteins transcribed by NEP and/or PEP in these plants in relation to control specimens (Figure 4). *psaA*, *psbA*, *psbK*, and *rbcL* were selected as PEP-dependent genes (class I), *accD*, *rpoA*, and *rpoB* were selected as NEP-dependent genes (class III), and *clpP* and *ndhB* were chosen as class II genes. The analysis revealed a consistent decrease in mRNA levels of class I
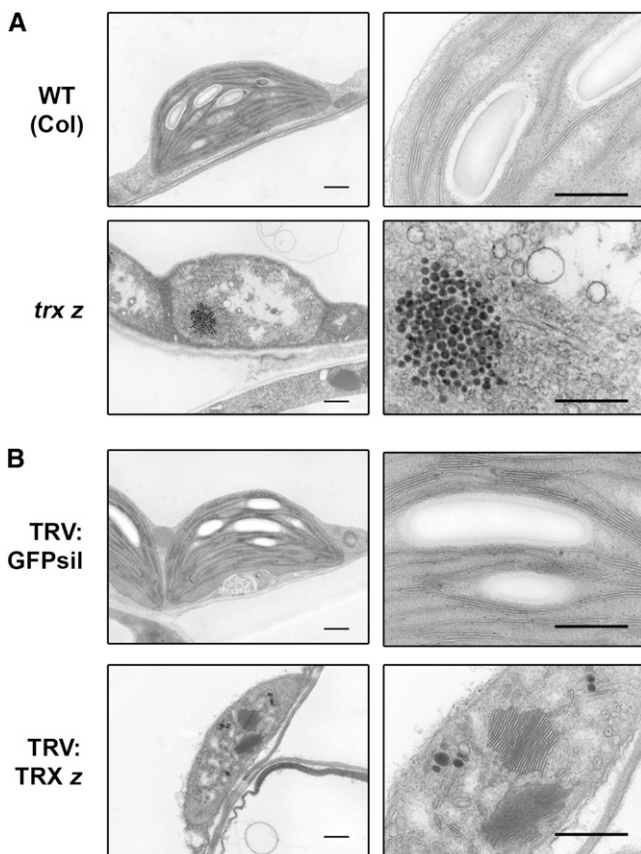
Figure 3. Transmission Electron Micrographs of Plastids in *Arabidopsis* and *N. benthamiana* Plants with Reduced TRX *z* Function.

(A) *Arabidopsis* wild type (WT; Col-0) and *trx z*.
(B) *N. benthamiana* TRV:TRX *z* versus TRV:GFPsil control.
Images on the right are a close-up of the same plastids shown on the left side. Bars = 0.5 μm.

genes, while transcript levels for class III genes were enhanced in both *trx z* and TRV:TRX *z* plants (Figure 4). For class II genes also, accumulation of mRNA was higher in plants with a loss of TRX *z* function. The expression of nuclear-encoded genes whose gene products are targeted to the chloroplast (*psaE*, *psaH*, *psaO*, *trx f1*, and *trx x*) was unaffected in both *trx z* and TRV:TRX *z* plants (Figure 4). This indicates that the changes in chloroplast gene expression observed are not due to a general effect on transcription. Taken together, these results suggest that TRX *z* is required for PEP-dependent transcription in chloroplasts.

Identification of TRX *z* Target Proteins Using the Yeast Two-Hybrid System

We next sought to identify possible TRX *z* target proteins using a yeast two-hybrid approach. To this end, the predicted mature TRX *z* protein ranging from amino acid 81 to 183 was used in fusion with the GAL4 BD as bait to screen two different two-hybrid cDNA libraries from different tissues of *Arabidopsis*. Of ~9 × 10^{7} primary transformants, 239 clones were selected for

being positive in growing on His-selective plates and additionally showing *LacZ* activity. From these, 85 clones were randomly chosen and further analyzed by DNA sequencing. Forty inserts encoded two different members of the pfkB-type carbohydrate kinase protein family (At3g54090, 16 times; At1g69200, 24 times). A conserved domain search revealed the presence of a fructo-kinase domain in both proteins (domain cd01167; Marchler-Bauer et al., 2009), and an alignment of the respective protein region of At3g54090 and At1g69200 to the fructokinase domain of FRK3, an experimentally confirmed fructokinase from tomato (German et al., 2004), showed a high degree of sequence conservation between the three proteins in this region (see Supplemental Figure 3 online). We therefore named At3g54090 FLN1 (fructokinase-like protein 1) and At1g69200 FLN2 (fructo-kinase-like protein 2).

The 16 FLN1 sequences consisted of three different clones starting with either amino acid 8, 12, or 20 of the predicted FLN1 polypeptide, while the FLN2 group consisted only of two different clones starting with residues 176 and 187, respectively. The specificity of the interaction between TRX *z* and the two FLNs was verified by retransforming the respective plasmids back into the yeast reporter strain in combination with either the bait plasmid BD-TRX *z* or control plasmids (Figure 5).

Coexpression of TRX z and FLNs in *Arabidopsis*

For the interaction to be relevant in vivo, both partners have to be expressed in the same tissue. Using the *Arabidopsis* coresponse
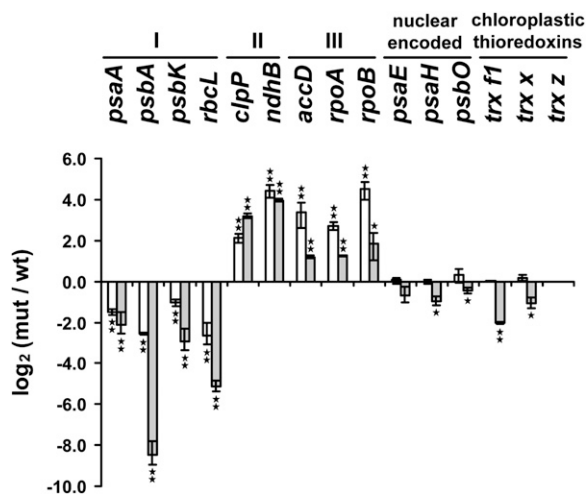

Figure 4. Changes in Transcript Abundance of Plastome-Encoded and Nucleus-Encoded Genes in *Arabidopsis trx z* and *N. benthamiana* TRV: TRX *z* Plants.

The $\log_2$ (mutant [mut]/wild type [wt]) value is given, where 3.32 corresponds to a 10-fold upregulation and -3.32 to a 10-fold downregulation in the mutant or transgenic plant relative to its control. n.d., not detectable. I, class I genes; II, class II genes; III, class III genes; white bars, TRV:TRX *z*; gray bars, *trx z*. Error bars indicate SD ($n = 3$). 18S rRNA was used as a reference. Significant differences between *Arabidopsis trx z*/TRV:TRX *z* plants and the respective control plants were calculated using Student's *t* test and are indicated by *P < 0.05 and **P < 0.01.
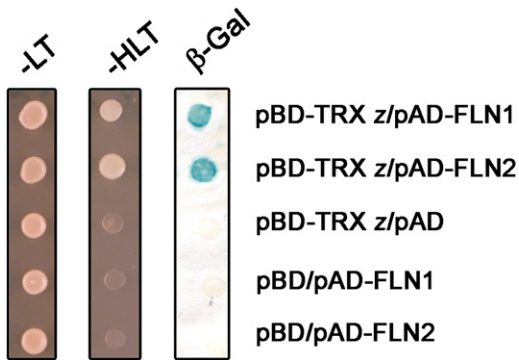
Figure 5. Interaction of TRX z with FLN1 and FLN2 in Yeast Two-Hybrid Assays.

The predicted mature TRX *z* protein fused to the GAL4 DNA binding domain (BD) was expressed in combination with either FLN1 (amino acids 8 to 471) or FLN2 (amino acids 176 to 616) fused to the GAL4 activation domain (AD) in yeast strain AH109. Cells were grown on selective media before a *lacZ* filter assay was performed. Empty BD and AD vectors served as negative controls. –LT, yeast growth on medium without Leu and Trp. –HTL, yeast growth on medium lacking His, Leu, and Trp, indicating expression of the *HIS3* reporter gene. β-Gal, activity of the *lacZ* reporter gene.
[See online article for color version of this figure.]

database (http://csdb.mpimp-golm.mpg.de; Steinhauser et al., 2004), we searched for transcriptional correlations using transcript profiles of all *Arabidopsis* tissues of the AtGenExpress developmental series (Schmid et al., 2005) and the nonparametric Spearman's Rho rank correlation (r_s), which ranges from +1 to −1 (the closer the correlation is to either +1 or −1, the stronger the relationship). The analysis revealed an exceptionally high degree of coexpression between TRX *z* and the two FLNs. The r_s for TRX *z* and FLN1 was 0.9497, and for TRX *z* and FLN2, it was 0.9490.

Subcellular Localization

FLN1 and FLN2 contained a putative N-terminal chloroplast-targeting sequence predicted by ChloroP (Emanuelsson et al., 1999). To confirm the localization of these proteins in plant cells, we generated constructs containing the full-length cDNA of FLN1 and FLN2, respectively, fused to the yellow fluorescent protein (YFP) at their C termini. Transient expression of FLN:YFP fusion proteins in epidermal cells of tobacco leaves by means of particle bombardment resulted in YFP fluorescence in discrete regions inside chloroplasts (Figure 6A). The fluorescent pattern of both FLNs inside chloroplasts resembles the appearance of nucleoids that are located within the stroma as small particles mostly associated with thylakoids. Hence, we analyzed whether FLN:YFP fluorescence was colocalized with cyan fluorescent protein (CFP) fused with PEND (for plastid envelope DNA binding), a well-characterized DNA binding protein in the inner envelope membrane of the developing chloroplast (Sato et al., 1993). In accordance with previously published data, fluorescence signals of PEND:CFP were observed in the cell nucleus

and chloroplast nucleoids (Figure 6B). An overlay with FLN:YFP fluorescence shows colocalization with PEND:CFP signals in the chloroplast, indicating that both FLN1 and FLN2 colocalized with nucleoids in leaf chloroplasts (Figure 6B).

TRX *z* Interacts with FLN1 and FLN2 in Planta

To investigate the association of TRX *z* and the FLNs in planta, a bimolecular fluorescence complementation (BiFC) assay was performed in *N. benthamiana* plants using transient expression via particle bombardment (Walter et al., 2004). The entire coding region of TRX *z* was fused to the C-terminal YFP fragment (YFP^C), whereas the coding regions of FLN1 and 2 were individually fused with the N-terminal YFP fragment (YFP^N). Pairwise expression of unfused YFP^N and YFP^C or their combination with the respective FLN fusions induced no YFP fluorescence (see Supplemental Figure 4 online). By contrast, strong YFP fluorescence was observed when combinations of TRX *z* and FLN1 or FLN2 were expressed, demonstrating TRX *z*/FLN complex formation in plant cells (Figure 6C). Similar to the fluorescence pattern observed for the FLN:YFP fusion proteins, the YFP signal in TRX *z*/FLN BiFC experiments was also detected in specific regions inside the chloroplast most likely representing nucleoids (Figure 6B). Taken together, these results strongly support the hypothesis that TRX *z* and FLNs interact inside chloroplast and function in chloroplast nucleoids.

Formation of Mixed Disulfides between TRX *z* and FLNs

The Cys residues in the active site of TRXs enable them to reduce other Cys-containing proteins. When these Cys residues are in the reduced form, the first Cys in the TRX active site (Cys-106 in TRX *z*) can form a mixed disulfide with the target protein. This intermolecular disulfide bond is quickly reduced by the second Cys (Cys-109 in TRX *z*), resulting in release of the reduced target protein from the oxidized TRX. However, TRXs can also bind to other proteins by electrostatic interactions, possibly enabling the interacting protein to achieve an optimal conformation (Balmer et al., 2004a). To investigate the role of the active-site Cys residues in mediating the interaction of TRX *z* with the FLNs, Cys-106 and Cys-109 were individually mutated to Ser by site-directed mutagenesis. Subsequently, the ability of the mutated TRX *z* variants to bind to FLNs was analyzed in yeast using a quantitative β-galactosidase assay. If binding of TRX *z* to FLN is thiol dependent, the Cys-106 to Ser mutation should weaken the interaction, whereas the substitution of Cys-109 by Ser should not affect the formation of a mixed disulfide between TRX and a given target protein. As shown in Table 1 the Cys$_{106}$Ser mutation strongly reduced the interaction strength of TRX *z* with both FLNs compared with the wild-type TRX *z*, indicating that TRX *z* binding to FLNs involves the formation of a mixed disulfide. Accordingly, the Cys$_{109}$Ser substitution left the interaction strength unaffected. These results clearly demonstrate that binding of TRX *z* to the two FLNs is thiol dependent and not solely mediated by electrostatic interactions and thus fulfils one of the requirements for a true TRX–target protein interaction.
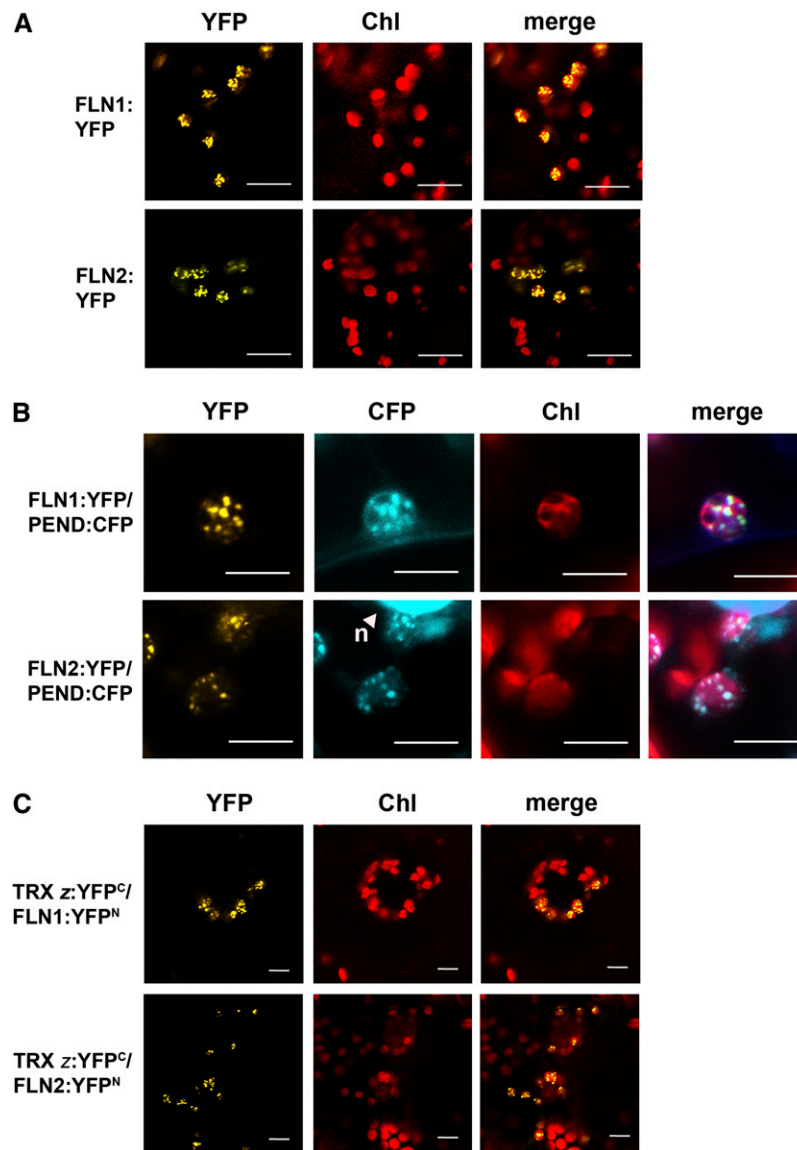
Figure 6. Subcellular Localization of FLN Proteins and TRX *z*–FLN Interaction.

(A) Subcellular localization of FLN1:YFP and FLN2:YFP fusions in tobacco leaves transiently transformed by particle bombardment. The yellow fluorescence of YFP (left) and the red autofluorescence of chlorophyll (Chl, middle) were monitored separately, and the two fluorescence images were merged (right). Bars = 10 μm.

(B) Colocalization of FLN:YFP fusion proteins (yellow) and PEND:CFP (blue) with chloroplast nucleoids. The arrowhead indicates the large fluorescent spot that represents the nucleus (n) of a guard cell. Bars = 10 μm.

(C) Visualization of protein interactions in plastids by the BiFC assay. YFP confocal microscopy images show tobacco leaf epidermal cells transiently expressing constructs encoding the fusion proteins indicated. Merge indicates an overlay of the YFP and chlorophyll autofluorescence images. Each image is representative of at least two experiments. Bars = 10 μm.

Identification of Essential Cys Residues in TRX *z* Target Proteins

To validate FLN1 and FLN2 as TRX target proteins, we sought to identify conserved Cys residues in their primary structures. An alignment of FLN1 and FLN2 sequences identified in other plant species revealed the presence of a double Cys motif conserved throughout the 18 sequences analyzed (see Supplemental Figure

5 online). With respect to the *Arabidopsis* FLNs, the double Cys motif is located at positions 105 and 106 in FLN1 and at 208 and 209 in FLN2. To assess the role of individual Cys residues in mediating TRX *z*–FLN interaction, we performed site-directed mutagenesis. Three mutated variants of each FLN were fused to the GAL 4 activation domain and further assayed for interaction with BD-TRX *z* by quantitative β-Gal measurements.

Table 1. Summary of the Quantitative β-Galactosidase Measurement in Yeast Two-Hybrid Assays

Plasmid pGBT9 Containing GAL4 BD	Plasmid pAD-GAL4 Containing GAL4 AD	β-Galactosidase Activity (Miller Units)
TRX *z*	FLN1	31.11 ± 1.9
TRX *z*^C106S	FLN1	3.33 ± 0.2
TRX *z*^C109S	FLN1	35.34 ± 0.7
TRX *z*	FLN2	183 ± 19.3
TRX *z*^C106S	FLN2	92.5 ± 2.3
TRX *z*^C109S	FLN2	190 ± 1.4
TRX *z*	pAD	n.d.
TRX *z*^C106S	pAD	n.d.
TRX *z*^C109S	pAD	n.d.
TRX *z*	FLN1	54 ± 3.2
TRX *z*	FLN1^C105A	63.8 ± 1.9
TRX *z*	FLN1^C106A	5.9 ± 0.1
TRX *z*	FLN1^C105A/C106A	n.d.
TRX *z*	FLN2	149 ± 0.5
TRX *z*	FLN2^C208A	42.7 ± 2.6
TRX *z*	FLN2^C209A	47 ± 3.1
TRX *z*	FLN2^C208A/C209A	n.d.
pGBT9	FLN1	n.d.
pGBT9	FLN2	n.d.

The β-galactosidase activity using ONPG as a substrate is expressed in Miller units. The values represent the mean of an assay performed in triplicate ± SD. n.d., not detectable.

The Cys$_{105}$Ala mutation in FLN1 did not affect the interaction with TRX *z*, whereas the Cys$_{106}$Ala substitution reduced TRX *z* binding by ~90% as judged from a reduction in β-Gal activity (Table 1). In case of FLN2, the picture was slightly different as each Cys to Ala mutation within the double Cys motif had a similar effect on interaction strength; they both reduced β-Gal activity by ~70% (Table 1). Only when both consecutive Cys residues were mutated at the same time was the interaction between either FLN or TRX *z* completely abolished (Table 1). This indicates that the two consecutive conserved Cys residues within the FLN protein sequence play an important role in the formation of a mixed disulfide with TRX *z*. Moreover, loss of one Cys at this position may be partially compensated for by the remaining residue.

FLN1 and FLN2 in Planta Analyses

If the FLNs were the main regulatory target proteins for TRX *z*, we anticipated that a reduction of FLN expression would lead to similar phenotypic effects, as previously observed for a loss of TRX *z* function. An inspection of the respective databases failed to identify an obvious insertional mutant for either of the two *Arabidopsis* FLN proteins at the time of these studies. Therefore, we created transgenic *Arabidopsis* plants expressing either a FLN1 or a FLN2 RNA interference construct under control of an ethanol-inducible promoter (iRNAi). In addition, the TRV VIGS system was used to silence the FLN1 and FLN2 orthologs individually in *N. benthamiana*.

Four to six days after induction with ethanol, *Arabidopsis* FLN1 and FLN2 RNAi plants displayed partial chlorosis that

was first visible in the top leaves and also appeared in nascent leaves that developed after induction (Figure 7A). Leaves that developed after agroinfection of TRV:FLN1 *N. benthamiana* plants were severely bleached 14 d after induction. Virus-mediated silencing of FLN2 affected leaf pigmentation only very mildly (Figure 8A). The phenotypic changes were in all cases restricted to very young leaves or leaves that emerged after the respective treatment. Leaves that were fully developed at the time of ethanol induction or agroinfection never displayed chlorosis.

Given the strong phenotype of TRV:FLN1 *N. benthamiana* plants, we again used transmission electron microscopy to investigate morphological changes in the plastids of these
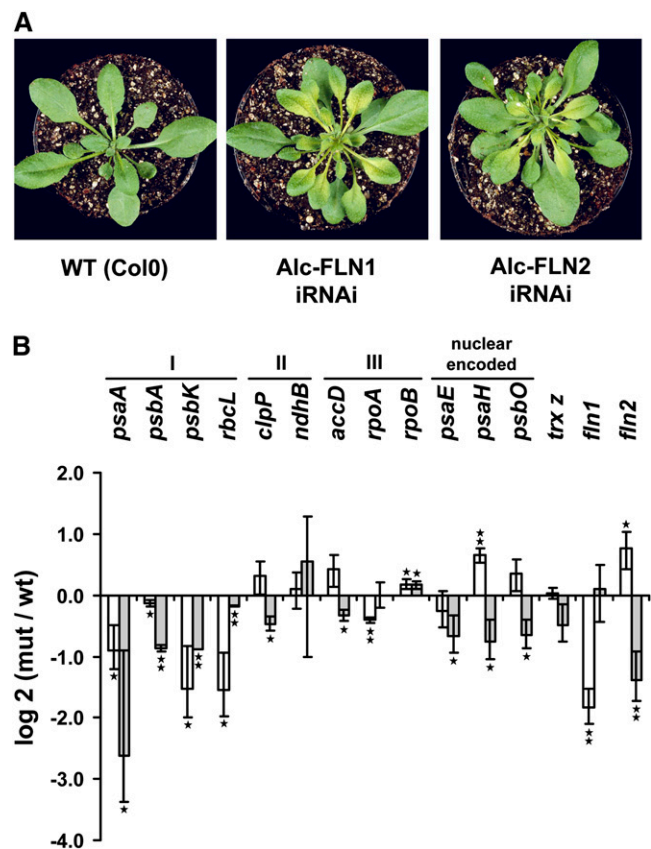

Figure 7. Silencing of *FLN1* and *FLN2* in *Arabidopsis* Using Ethanol-Inducible RNAi.

(A) Phenotype of transgenic *Arabidopsis* plants 5 d after ethanol treatment compared with the wild-type (WT) control.
(B) Changes in transcript abundance of plastome-encoded and nucleus-encoded genes in *Arabidopsis* FLN1 and FLN2 iRNAi plants. The log$_2$ (mutant [mut]/wild type [wt]) value is given, where 3.32 corresponds to a 10-fold upregulation and −3.32 to a 10-fold downregulation in the iRNAi plants relative to the wild type. n.d., not detectable. I, class I genes; II, class II genes; III, class III genes; white bars, iRNAi FLN1; gray bars, iRNAi FLN2. Error bars indicate SD (n = 3). 18S rRNA was used as a reference. Significant differences between *Arabidopsis* iRNAi FLN plants and the wild type were calculated using Student's *t* test and are indicated by *P < 0.05 and **P < 0.01.
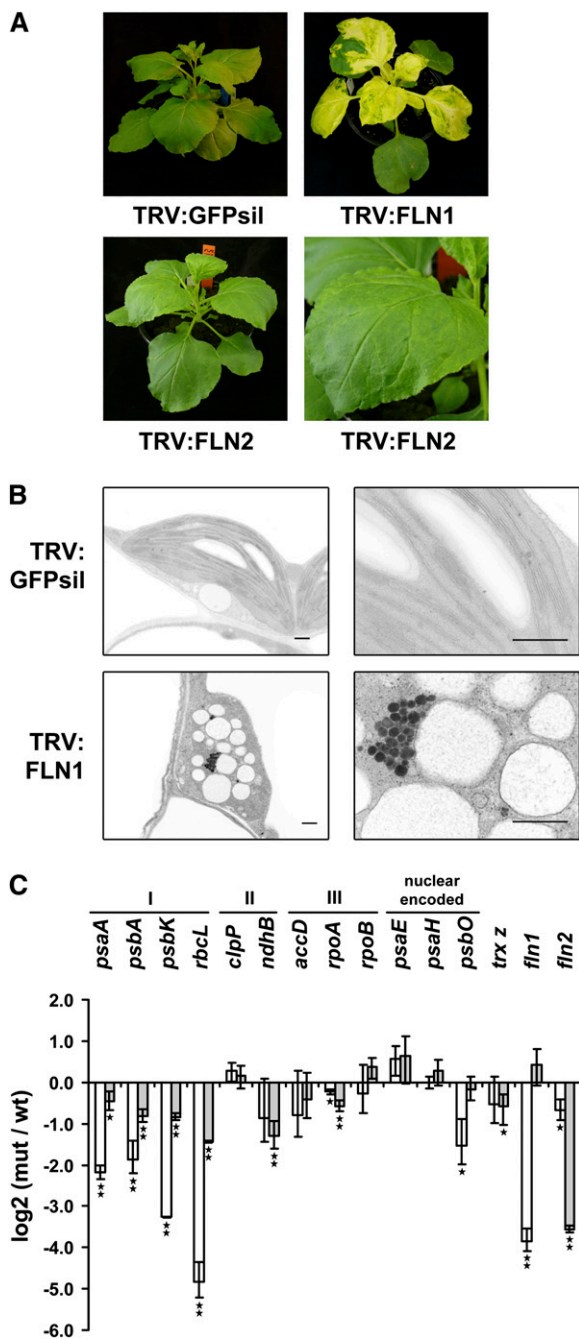
Figure 8. Silencing of *FLN1* Expression in *N. benthamiana* Using TRV-Based VIGS.

(A) Phenotype of *N. benthamiana* FLN-1 (top right) and FLN-2 (bottom) VIGS plants in comparison to the TRV:GFPsil control.

(B) Transmission electron micrographs of plastids from *N. benthamiana* VIGS FLN1 plants (TRV:FLN1). Bars = 0.5 μm.

(C) Changes in transcript abundance of plastome-encoded and nucleus-encoded genes in *N. benthamiana* FLN-1 and FLN-2 VIGS plants. The log$_2$ (mutant [mut]/wild type [wt]) value is given, where 3.32 corresponds to a 10-fold upregulation and −3.32 to a 10-fold downregulation in the VIGS FLN plants compared with the control. n.d., not detectable. I, class I genes; II, class II genes; III, class III genes; white bars, VIGS FLN1; gray

bars, VIGS FLN2. Error bars indicate SD (*n* = 3). 18S rRNA was used as a reference. Significant differences between FLN1/FLN2 VIGS plants and control plants were calculated using Student's *t* test and are indicated by *P < 0.05 and **P < 0.01.

plants. As shown in Figure 8B, the plastids in tissues taken from phenotypic leaves of TRV:FLN1 plants were highly vacuolated and lacked internal membrane structures, such as single stromal thylakoids or stacked grana thylakoids, and they contained abnormal suborganelle structures. In addition, there was a considerable number of densely stained globular structures, probably plastoglobuli.

Quantitative real-time RT-PCR analysis of chloroplast gene expression in phenotypically affected leaves revealed a consistent downregulation of PEP-dependent class I genes in *Arabidopsis* iRNAi FLN plants as well as in TRV:FLN *N. benthamiana* plants (Figures 7B and 8C). By contrast, transcript levels of NEP-dependent class III genes, as well as of class II and nuclear-encoded genes, were not consistently affected by a reduction of FLN expression with only a few exceptions in TRV:FLN1 plants (Figure 8C). In agreement with the phenotypic differences between TRV:FLN1 and TRV:FLN2 *N. benthamiana* plants, suppression of FLN2 affected class I transcript levels much less than did suppression of FLN1, although the reduction in *FLN* transcript itself was comparable between both types of plants (Figure 8C). Taken together, these data suggest that FLN1 and FLN2 are involved in PEP-dependent transcription in plastids in a way similar to that observed for their interaction partner TRX *z*.

Recombinant FLNs Lack Detectable Fructokinase Activity

To investigate FLN1 and FLN2 function on the biochemical level, both predicted mature proteins were produced in *E. coli* as a fusion to the maltose binding protein and purified by affinity chromatography using amylose resin. As a control protein, we included FRK3 (At1g66430), an *Arabidopsis* ortholog of tomato fructokinase 3, which has been shown to be a plastidic fructokinase (German et al., 2004; Damari-Weissler et al., 2006). Whereas enzymatic activity for MBP-AtFRK3 was readily detectable, neither of the two recombinant MBP-FLN fusion proteins showed detectable fructokinase activity (see Supplemental Figure 6 online). The addition of 50 mM DTT alone or in combination with recombinant TRX *z* protein prior to the enzyme measurement did not yield detectable enzymatic activity, indicating that both recombinant FLNs do not possess redox-dependent fructokinase activity (see Supplemental Figure 6 online). Phylogenetic analyses were conducted to gain further insights into the evolutionary origins and possible functions of the FLNs (see Supplemental Figure 7 online). These showed that both FLN1 and FLN2 are conserved in monocotyledonous and dicotyledonous angiosperms, but in the moss *Physcomitrella patens*, only FLN1 is present. No close homologs were found in various bacterial and yeast genomes, suggesting that the FLNs first evolved in the green plant lineage and predate the appearance of vascular plants. Their close phylogenetic relationship with known fructokinases indicates that the FLNs may have evolved from an active FRK or that they share a common

ancestor with the FRKs. Protein sequence alignment between plant fructokinases for which enzymatic activity has been reported and FLNs revealed a noticeable sequence divergence within the pfkB signature motif II, an amino acid stretch that has been implicated as playing a role in substrate and/or cofactor binding in this enzyme family (Sigrell et al., 1998; Miallau et al., 2007). All enzymatically active fructokinases from plants described so far contain a conserved motif II (DTTGAGD), whereas this motif has been altered to DRTGSGD in FLN1 and DMSA/QSGD in FLN2 (see Supplemental Figure 5 and Supplemental Figure 8 online). Members of the pfkB family of carbohydrate kinases phosphorylate a range of sugar substrates. Therefore, we employed thin layer chromatography to investigate FLN sugar phosphorylating activity using galactose, mannose, psicose, tagatose, and xylose as substrates. However, none of these sugars appeared to be phosphorylated by recombinant FLN1 or FLN2 (data not shown). Taken together, these results make it at least questionable that FLN1 and FLN2 are functional sugar kinases in vivo.

The in Planta Redox State of FLN2 Is Modulated by Light/Dark Transitions in a TRX *z*–Dependent Manner

Finally, we sought to assess the in planta redox state of FLN2 by visualizing changes in protein mobility in nonreducing SDS-PAGE using an FLN2-specific antibody. To investigate the role of TRX *z* in FLN2 reduction, wild-type and *trx z Arabidopsis* mutant plants were analyzed. Samples were taken from leaves of agar grown plants either during the light or after 1 h of darkening. As shown in Figure 9, under reducing conditions, a clear band matching the expected size of the mature FLN2 protein could be detected in wild-type and *trx z* plants independent of whether the samples were taken during the light or after darkening. This

Figure 9. The in Planta Redox State of FLN2 Is Modulated by Light/Dark Transitions in a TRX *z*–Dependent Manner.

Leaf material was harvested from *Arabidopsis* Col-0 wild-type (WT) or *trx z* mutant plants either during the light (L) or after 1 h of darkening (D). Samples were subjected to either reducing (+DTT) or nonreducing (−DTT) SDS-PAGE, and the FLN2 protein was detected using a FLN2-specific antibody (top panel). The position of the FLN2 band is indicated by an arrow. The asterisk marks a nonspecific cross-reacting band. An identically loaded gel was run in parallel and stained with Coomassie blue as a loading control (bottom panel). The figure shows a representative result of three repetitions using independent biological material.

indicates that FLN2 was expressed to a similar level in both genotypes and under both conditions. The picture changed when the same samples were run under nonreducing conditions (Figure 9). The FLN2-specific band in wild-type plants was readily detectable in samples taken during illumination, whereas the signal intensity was greatly reduced in dark treated samples. This strongly suggests that the redox state of FLN2 is regulated in vivo by a change of the redox environment in chloroplasts during light/dark transitions. In samples taken from wild-type plants in the light, the FLN2 band runs slightly slower than in the same samples taken from darkened leaves. This was true under reducing and nonreducing conditions and might indicate that FLN2 undergoes an additional posttranslational modification (e.g., phosphorylation) following reduction in the light. Indeed, an inspection of the PhosPhAt database (http://phosphat.mpimp-golm.mpg.de; Durek et al., 2010) revealed a possible phosphorylated Ser either at position 131 or 132 of the FLN2 polypeptide. Unexpectedly, no additional band indicative of an oxidized form of FLN2 migrating at a size different from the reduced form could be detected in the immunoblots from nonreducing SDS-PAGE. This could either be due to the inability of the FLN2 antibody to detect the oxidized form of FLN2 or because oxidized FLN2 builds higher molecular weight complexes that do not migrate into the gel. When analyzed under nonreducing conditions, no FLN2 band could be detected in samples taken from *trx z Arabidopsis* plants independent of whether the material was harvested during illumination or after darkening (Figure 9). This clearly indicates that in vivo changes of the FLN2 redox state during light/dark transitions are predominantly mediated by TRX *z*.

DISCUSSION

The TRX system is particularly complex in higher plants, involving numerous isoforms present in various cellular compartments. The chloroplast system with four types of TRX, 2*f*, 4*m*, 1*x*, and 2*y*, is the best documented; nevertheless, the exact function of each isoform remains unclear (Gelhaye et al., 2005; Meyer et al., 2005, 2008). The characterization of TRX *z* in this study raises the total number of plastidial TRXs in *Arabidopsis* to 10. The tomato ortholog of TRX *z* (named CITRX) has recently been shown to interact with the cytoplasmic C terminus of the Cf-9 resistance protein in a yeast two-hybrid screen and was characterized as a negative regulator of defense against specific races of the fungal pathogen *Cladosporium fulvum* (Rivas et al., 2004). It was further shown that CITRX/Sl-TRX *z* also binds to ACIK1, a protein kinase involved in defense signaling, and thus might serve as an adaptor protein mediating the interaction between the cytoplasmic domain of Cf-9 and ACIK1 upon perception of Avr9 (Nekrasov et al., 2006). Interestingly, the interaction of CITRX/Sl-TRX *z* with Cf-9 as well as with ACIK1 was independent of a functional TRX active site, and catalytic activity of CITRX/Sl-TRX *z* was found to be dispensable for the attenuation of the Cf-9/Avr9-induced defense response in tomato (Nekrasov et al., 2006). Rivas et al. (2004) reported the interaction with Cf-9 to take place in the cytosol of the plant cell and thus propose that CITRX/Sl-TRX *z* is a cytosolic protein.
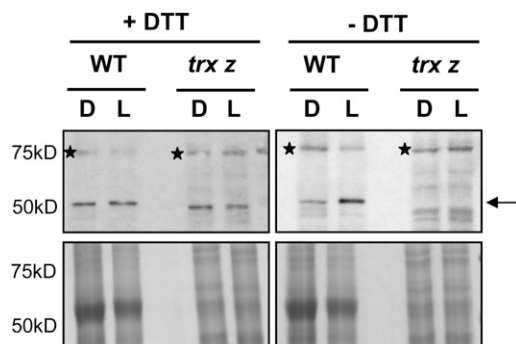
However, no biochemical data on the localization of the protein are presented, and moreover ChloroP (Emanuelsson et al., 1999) predicts a chloroplast transit peptide also for the tomato protein (score 0.557). This makes a predominant cytosolic localization of the CITRX/Sl-TRX *z* at least questionable, although recruiting of a plastidial protein to the cytosol during pathogen defense has recently been shown to occur during the interaction of tobacco with TMV (Caplan et al., 2008). Although CITRX/Sl-TRX *z* appears to possess a redox-independent function in Cf-9–mediated disease signaling in tomato, TRX *z* likely has other functional roles in plants, including in those that are nonhosts of *C. fulvum.*

Loss of *TRX z* expression in an *Arabidopsis* T-DNA insertion mutant or VIGS of *TRX z* in *N. benthamiana* plants induces strong phenotypic changes, including pale-green leaves, and microscopy analysis revealed marked disruption of proper development of the plastid. Genetic approaches to characterize TRXs in planta have rarely been successful, most likely owing to functional redundancy of individual isoforms within *TRX* gene families. The phenotype of plants with a loss of or reduced *TRX z* expression suggests that this particular TRX isoform holds a specificity that is not shared by other TRXs; thus, its loss cannot be compensated for. It was recently reported that TRX *z* is a component of TACs isolated from plastids from *Arabidopsis* and mustard (Pfalz et al., 2006). In that study, 18 new plastid transcriptionally active chromosome proteins (pTACs) could be identified, and three of those (pTAC-2, - 6, and -12) were shown by analysis of the corresponding *Arabidopsis* T-DNA mutants to be essential for autotrophic growth. Homozygous *ptac* knockout mutants developed white cotyledons. On sucrose-containing medium, *ptac2* develops yellow cotyledons and greenish primary leaves, whereas the leaves of the other two mutants are more yellowish. Thus, *ptac* mutants phenotypically resemble *trx z* T-DNA mutants and TRV:TRX *z N. benthamiana* VIGS plants. The expression pattern of plastid genes in the *ptac* mutants is identical to those of *Δrpo* mutants and mutants that do not accumulate PEP. All of these show a downregulation of class I plastid genes with PEP promoters, while the expression of class III genes with NEP promoters is upregulated. The similarities between PEP-deficient mutants and plants with a loss of or reduction in *TRX z* expression strongly suggest that TRX *z* is a functional component of the PEP complex and that it functions in plastid gene expression. The reason for the observed upregulation of NEP-dependent class III genes in these plants is unclear. NEP is largely responsible for the transcription of housekeeping genes during early chloroplast development (Hajdukiewicz et al., 1997). Subsequent light-dependent chloroplast maturation is accompanied by repression of NEP activity and activation of PEP. Recent work suggests that this switch in RNA polymerase usage is mediated by the plastid-encoded tRNA[Glu] whose expression depends on PEP and directly binds to and inhibits the transcriptional activity of NEP (Hanaoka et al., 2005). Compromised PEP activity in plants with reduced TRX *z* function would lead to a decrease in tRNA[Glu] expression, thus preventing inhibition of NEP and eventually leading to higher class III gene expression compared with control plants with normal PEP activity.

The finding that expression of a selected set of nuclear-encoded chloroplast-localized proteins is not consistently changed in plants with reduced TRX *z* function is puzzling in the light of the general assumption that organellar and nuclear gene expression systems are tightly coordinated. This coordination requires signaling from the plastid that conveys information on its developmental and metabolic state to the nucleus (retrograde signaling), thus enabling nuclear gene expression to be modified in accordance with the status of the chloroplast (Nott et al., 2006; Pogson et al., 2008). Plastid gene expression (PGE) has previously been identified as one of the factors able to generate a retrograde signal in such a way that inhibiting PGE has strong effects on expression of specific nuclear-encoded genes. *Arabidopsis* GUN (genomes uncoupled) loci have been identified as components of plastid-to-nucleus signal transduction (Susek et al., 1993; Mochizuki et al., 2001). Unlike wild-type plants, *gun* mutants have nuclear *Lhcb1* expression in the absence of chloroplast development. One mutant, *gun1*, shows *Lhcb1* expression in plants treated with plastid translation inhibitors, thereby implicating GUN1 in PGE-dependent retrograde signaling (Nott et al., 2006). GUN1 has recently been cloned (Koussevitzky et al., 2007) and shown to encode a pentatricopeptide repeat–containing protein with highest similarity to PTAC-2 (Pfalz et al., 2006). Given the similarities between the *ptac-2* mutant and the plants with reduced *TRX z* expression, it is tempting to speculate that generation of a PGE signal might depend on an intact plastid-encoded transcriptional complex, and loss of PEP function thus could eliminate initiation of this plastid signal, similar to a loss of the GUN1 protein as in the *gun1* mutant. However, to establish whether plants with reduced TRX *z* function exhibit a true GUN phenotype requires a more detailed analysis.

Since TRX is not known as a DNA binding protein, it appears likely that TRX *z* would act on the regulation of plastid transcription indirectly by thiol modification of another PEP component. In mammals, TRXs are implicated in a redox regulation of transcription factors such as NF-κB or AP-1 (Schulze-Osthoff et al., 1995). More recently, TRX was also shown to be involved in the oxygen-dependent regulation of photosynthesis genes encoded by the *puf* operon in *Rhodobacter sphaeroides* (Pasternak et al., 1999). Reduced TRX-A of *R. sphaeroides* interacts with DNA gyrase in a thiol-independent manner and alters its DNA supercoiling activity, thereby affecting gene expression (Li et al., 2004). Available evidence suggests that PGE is also under redox control in higher plants (Pfannschmidt and Liere, 2005). The transcription rate of specific chloroplast genes has been shown to be affected by the spectral quality of light (photosystem I [PSI] versus photosystem II [PSII] excitation) as part of an acclimatory response called photosystem stoichiometry adjustment. The function of photosystem stoichiometry adjustment is to compensate for any deficiency in energy conversion at either PSI or PSII by increasing the quantity of the photosytem that will otherwise become rate limiting to overall photosynthesis. In different plant species, it could be shown that this response is regulated by the redox state of the plastoquinone (PQ) pool via mechanism in which the expression of the two core proteins of the two photosystems is oppositely regulated (Pfannschmidt et al., 1999). Under conditions resulting in a reduced PQ pool (PSII light), transcription of *psaAB* (encoding the P700 apoproteins A and B of PSI) is enhanced, whereas this occurs for *psbA* (encoding the D1 protein of PSII) under conditions leading to

an oxidized PQ pool (PSI light). The signal transduction from the PQ pool to the level of transcription is not entirely clear yet; however, current models suggest involvement of phosphorylation cascades in redox regulation of PGE during photosystem stoichiometry adjustment. Recently, a chloroplast sensor kinase (CSK) has been identified that has been implicated in redox regulation of PGE (Puthiyaveetil et al., 2008). *Arabidopsis* CSK knockout mutants display a severe disturbance in *psaA* transcript accumulation during the photosystem stoichiometry adjustment, indicating that CSK is essential for proper redox regulation of *psaA* transcription, although the CSK target proteins yet remain elusive. However, recent evidence suggests that redox regulation of *psaA* and *psbA* transcription involves thiol modification acting synergistically with phosphorylation (Steiner et al., 2009), implicating a role for TRXs in this process. TRX *z* could thus play a role in mediating redox signals in photosystem stoichiometry adjustment as a long-term response to fluctuating light conditions. Alternatively, TRX *z* could link PEP function more directly to photosynthetic electron transport (PET). In addition to light quality, light intensity has also been shown to affect *psbA* transcription (Kettunen et al., 1997). In chloroplasts, TRXs can receive electrons either from the photosynthetic electron transport chain via ferredoxin/TRX reductase or from NADPH via NTRC. *Arabidopsis* NTRC knockout plants display a weak phenotype characterized by slow growth and pale-green leaves, especially under short-day conditions (Lepistö et al., 2009). From the distinct phenotypes of *ntrc* and *trx z* mutant lines, it might be concluded that NTRC is not an electron donor to TRX *z* and thus most likely receives electrons from PET. In the latter case, thiol modification by TRX *z* would be coupled to a light signal. Enhanced rates of plastid transcription by light have been reported in several species, including pea (*Pisum sativum*; Kettunen et al., 1997), barley (*Hordeum vulgare*; Baumgartner et al., 1993), and tobacco (*Nicotiana tabacum*; Shiina et al., 1998). Transcriptional changes during dark/light transitions have been attributed to light-induced PEP activity (Shiina et al., 1998), which may be brought about by TRX *z* mediated redox regulation.

To unravel the signal chain from TRX *z* to plastid transcription, we attempted to identify TRX *z* target proteins using a yeast two-hybrid approach. In contrast with the many putative TRX targets isolated through in vitro proteomics (Buchanan and Balmer, 2005), very few TRX target proteins have been isolated using TRXs as bait to screen two-hybrid DNA libraries (Nishiyama et al., 1999; Yamanaka et al., 2000; Brodegger et al., 2004; Vignols et al., 2005). The low efficiency of the yeast two-hybrid system to identify TRX target proteins has been attributed to the presence of functional endogenous TRXs in yeast that either compete with the foreign TRXs used as a bait or reduce the disulphide bond established in vivo between the TRX bait and its target protein (Verdoucq et al., 1999; Vignols et al., 2005). To circumvent this problem, Vignols et al. (2005) developed a yeast two-hybrid reporter strain carrying deletions in the endogenous yeast *TRX1* and *TRX2* genes. The authors could demonstrate that in the modified strain, yeast TRXs and *Arabidopsis* TRX introduced as a bait interacted with known partner proteins, whereas the same interactions could not be detected using a classical two-hybrid reporter strain (Vignols et al., 2005). In our study, we were able to identify two pfkB family fructokinase-like proteins (FLNs) as

putative TRX *z* targets. The specificity of the interaction could be confirmed in planta using BiFC. Obviously, endogenous TRXs were not able to interfere with the interaction in yeast, which might indicate a high specificity for TRX *z* binding to the FLNs. To the best of our knowledge, neither of the FLNs has been indicated as a putative TRX target protein identified through TRX affinity approaches. This either again argues for a very specific interaction of the FLNs with TRX *z* or for a very low abundance of FLNs in planta. Remarkably, just as for TRX *z*, both FLNs have been shown before to be components of TACs (Pfalz et al., 2006). In addition, FLN1 was also present in a highly purified PEP complex from tobacco chloroplasts (Suzuki et al., 2004). In accordance with these findings, FLN:YFP fusion proteins and TRX *z*–FLN interaction in BiFC assays localized to specific regions of the chloroplast whose locations correlated with PEND:CFP in plastid nucleoids. Taken together, the available data strongly suggest that both FLNs specifically bind to TRX *z* in vivo as part of a functional PEP complex.

Using Cys-to-Ser substitution in the TRX *z* active site, we were able to show that binding of TRX *z* to both FLNs involves the formation of a mixed disulfide between the first Cys of the CXXC active site and the target protein, which is consistent with the proposed TRX reaction mechanism. Further mutational analyses of conserved Cys residues within both FLN polypeptides revealed that two consecutive Cys residues ($Cys_{105/106}$ in FLN1 and $Cys_{208/209}$ in FLN2, respectively) are partially redundant in forming the mixed disulfide with TRX *z*, as only a double mutation of both Cys residues completely abolished the interaction. Although monitoring the in planta redox state of FLN2 using immunodetection under nonreducing versus reducing conditions revealed differences in the FLN2 redox state between light and dark treatment, the experiment did not provide a clear view about the size of the oxidized FLN2 protein. The weak double band appearing below the specific FLN2 band in dark-treated samples from the wild type might represent the oxidized form of FLN2, especially as it appears stronger under nonreducing conditions compared with reducing conditions (Figure 9). This would argue for the formation of an intramolecular disulfide bridge under oxidizing conditions. However, in samples taken from *trx z* mutant plants, there are also very faint bands detectable under nonreducing conditions that migrate at a higher molecular weight than the reduced form of FLN2. This could argue for the formation of intermolecular disulfide bridges with other protein partners. Further experiments will have to address the question as to whether the FLN double Cys motif participates in the formation of an intramolecular disulfide bridge with another Cys within the polypeptide chain or whether FLNs form intermolecular disulfide bridges to generate homo- or heteromers.

The in planta analysis of both FLNs provides further evidence for their functional association with TRX *z*. Inducible silencing of FLN1 and FLN2, individually, in transgenic *Arabidopsis* plants induces a similar leaf phenotype as loss of TRX *z* function and leads to a reduced expression of PEP-dependent class I genes. The same is true for VIGS of *N. benthamiana* FLNs, and microscopy observation indicates that plastid development is markedly impaired in TRV:FLN1 plants, as was previously shown in *trx z* *Arabidopsis* and TRV:TRX *z* *N. benthamiana* plants. However, it appears that silencing of FLN2 generally has a weaker effect on

the reduction of class I gene expression than does silencing of FLN1. Furthermore, TRV:FLN2 *N. benthamiana* plants develop relatively mild phenotypic alteration compared with TRV:FLN1 plants. This might indicate that FLN1 and FLN2 have at least some functional specificity, in that a loss of FLN2 expression can be partially compensated for by FLN1, whereas FLN2 cannot sufficiently make up for reduced FLN1 expression.

Using nonreducing SDS-PAGE of extracts from wild-type and *trx z Arabidopsis* plants in combination with an FLN-specific antibody, we were able to show that the FLN2 redox state changes in vivo during light/dark transitions and that this change is mediated by TRX *z*. This again argues for a role of the TRX *z*/FLN2 redox module in coupling PET to PEP function and thereby adjusting transcriptional rates to light intensity. In addition, the results support the notion that TRX *z* receives its electrons from PET.

What might be the function of the FLNs in the PEP complex? It has previously been shown that FRK3, one of the four fructokinase isoforms found in tomato, localizes to plastids (Damari-Weissler et al., 2006). This fructokinase has been shown to be enzymatically active (German et al., 2004). A putative ortholog of Sl-FRK3 can be identified in the *Arabidopsis* genome, and we were able to demonstrate enzymatic activity of the recombinant MBP-AtFRK3 protein. The localization of an active fructokinase in plastids raises questions about the source of fructose within these organelles. By contrast, all attempts to detect enzymatic activity of the two FLNs identified in our studies so far failed. The pfkB family of sugar kinases comprises proteins with diverse ATP-dependent sugar phosphorylation specificities, such as for ribose, adenosine, or fructose, among others (Bork et al., 1993; Ronimus and Morgan, 2001). Although there is a possibility that both FLNs have an enzymatic activity other than phosphorylating fructose, we currently favor the hypothesis that during evolution both proteins acquired a new function in plastid transcription. Indirect support for this is provided by the amino acid substitutions in the active site (Sigrell et al., 1998; Miallau et al., 2007). A similar hypothesis has recently been put forward for At-MurE, a protein whose bacterial counterpart catalyzes the ATP-dependent formation of uridine diphosphate-*N*-acetylmuramic acid-tripeptide in bacterial peptidoglycan synthesis. At-MurE was identified as a pTAC or PEP component in the same studies as TRX *z* and both FLNs (Suzuki et al., 2004; Pfalz et al., 2006), and RT-PCR analysis of At-MurE knockout mutants has demonstrated an essential role of the protein in PEP-dependent transcription (Garcia et al., 2008). Again, no enzymatic activity could be detected for At-MurE (Garcia et al., 2008). Other examples show that metabolic enzymes can play a role in transcriptional regulation in addition to their enzymatic function. For instance, plastidic sulfite reductases have DNA binding and DNA-compacting abilities that regulate plastid gene expression in addition to exhibiting sulfite reductase activity (Sekine et al., 2002, 2007).

Future studies will have to investigate whether FLNs are also able to bind DNA and if this activity might be redox dependent. Alternatively, FLNs could interact with other proteins of the PEP complex, which is indeed likely as at least FLN1 was identified as a component of affinity-purified plastid PEP complex, arguing for a tight association between FLN1 and the PEP core subunits

(Suzuki et al., 2004). This will be further tested by investigating direct protein–protein interactions of FLNs with PEP core subunits.

In conclusion, our data suggest that TRX *z* and the two FLNs might act as part of a signaling chain involved in the redox regulation of PEP function in chloroplasts and thus might link transcriptional regulation via PET to light signals.

METHODS

Plant Growth Conditions and Genetic Analysis

Arabidopsis thaliana seeds were sown on Murashige and Skoog (MS) agar (Sigma-Aldrich) plates supplemented with 2% (w/v) sucrose and cultivated in tissue culture under a 16-h-light/8-h-dark regime (irradiance 150 μmol quanta m^{-2} s^{-1}) at 50% humidity. *Arabidopsis* ecotype Columbia (Col) was used. The single insert *trx z* (Salk_028162) T-DNA *Arabidopsis* insertion mutant was obtained from the Nottingham Arabidopsis Stock Center (Nottingham University) and confirmed by PCR-based genotyping using the primers listed in Supplemental Table 1 online. *Nicotiana benthamiana* seeds were germinated on soil and cultivated in the greenhouse under a light/dark regime of 16 h light (25°C) and 8 h dark (20°C).

Construction of the 35S:*TRX z* Plasmid

The entire coding region of *TRX* z was amplified by PCR from *Arabidopsis* cDNA using the primers indicated in Supplemental Table 1 online. The PCR fragment was subcloned into pENTR-D/TOPO (Invitrogen) and subsequently recombined into the binary vector pB2GW7 (Karimi et al., 2002) using L/R-Clonase (Invitrogen). The resulting construct was designated p35S:*TRX z* and used to transform heterozygous *TRX z/trx z Arabidopsis* plants using floral dip transformation (Clough and Bent, 1998).

Fusion Gene Constructs

For subcellular localization studies of TRX *z*, the portion of the sequence encoding the predicted signal peptide (amino acids 1 to 81) was amplified by PCR using the primers listed in Supplemental Table 1 online. The resulting PCR product was inserted into the vector pENTR-D/TOPO (Invitrogen). To generate a translational fusion between the TRX *z* TP and GFP, the fragment was subsequently recombined into the destination vector pK7WGF2 (Karimi et al., 2002) using L/R-Clonase (Invitrogen). Using a similar strategy, the entire coding sequences of *FLN1* and *FLN2* were amplified by PCR and individually inserted into pENTR-D/TOPO. As the destination vector, a Gateway system–compatible version of the pFF19-YFP vector (Wachter et al., 2005) was used. For the PEND:CFP construct, a DNA fragment encoding the N-terminal region of PEND (88 amino acids) was amplified from genomic DNA and inserted into pFF19-CFP. Primers used for cloning of the above mentioned fragments are shown in Supplemental Table 1 online. A pBIN19 derivative carrying a cauliflower mosaic virus 35S–driven GFP was used as free GFP control (Brigneti et al., 1998).

Microscopy Analysis

Subcellular localization of several TRX *z* and FLN fusion proteins was analyzed using GFP, YFP, and CFP fluorescence. Tobacco (*Nicotiana tabacum* var Samsun NN) leaves were transiently transformed with the respective constructs by particle bombardment using a Bio-Rad PDS-1000 He particle delivery system according to the manufacturer's

instructions. GFP, YFP, and CFP fluorescence was observed by confocal laser scanning microscopy (Leica TCS SP2). Double-labeled cells were scanned sequentially to prevent any crosstalk between fluorescence channels. For transmission electron microscopy, images were obtained as described (Börnke et al., 2002).

BiFC Assay

Entry clones of FLN1 and FLN2 in pENTR-D/TOPO comprising the entire coding region of each cDNA were used in a L/R-reaction with a Gateway system–compatible version (Invitrogen) of the BiFC vector pUC-SPYCE (Walter et al., 2004). In the same way, the TRX z cDNA was inserted into the complementary BiFC vector pUC-SPYNE (Walter et al., 2004). Constructs were delivered into leaf cells of tobacco by particle bombardment using a Bio-Rad PDS-1000 He particle delivery system according to the manufacturer's instructions. The BiFC-induced fluorescence was detected by confocal laser scanning microscopy after 24 h of incubation at 22°C in the dark.

Generation of Transgenic *Arabidopsis* Plants

Constructs for ethanol-inducible RNA interference of *FLN1* and *FLN2* were generated as described (Chen et al., 2003) employing cDNA fragments amplified with specific primers listed in Supplemental Table 1 online. The resulting constructs were transformed into *Arabidopsis* using the floral dip method (Clough and Bent, 1998). For selection of transgenic plants, T1 seeds were surface sterilized and sown onto MS medium (Sigma-Aldrich) supplemented with Gamborg's vitamin solution (1:1000) and 50 μg of kanamycin per mL. Plants were given cold treatment for 2 d to synchronize germination before incubation under a 16-h-light/8-h-dark photoperiod (150 μM m^{-2} s^{-1} light, 21°C) at 50% relative humidity. Two weeks after germination, the plants were transferred to soil and further cultivated in the greenhouse for additional 9 d. Expression of the RNAi construct was achieved by root drenching the plants with 1% ethanol (750 mL per tray; 35 pots with single plants; 6-cm pot diameter).

Protein Expression in *Escherichia coli* and Activity Assays

For recombinant protein production, cDNAs of *FLN1*, *FLN2*, and *FRK3* from which the part encoding the predicted transit peptide had been removed were cloned into the pMal-c2 vector (New England Biolabs). The resulting plasmids were transformed into *E. coli* strain DH5a and the protein expressed as outlined in the instructions accompanying the pMal-c2 vector. Bacteria were lysed by sonication. After centrifugation, the recombinant proteins were purified using amylose resin and eluted using maltose. The purified proteins were analyzed by SDS-PAGE. For expression of recombinant TRX z in *E. coli*, the sequence encoding the predicted mature protein was amplified by PCR using the primers indicated in Supplemental Table 1 online. The forward primer was designed to introduce a His$_6$-tag at the 5′ end of the fragment. The PCR product was inserted into the pMal-c2 vector, and the recombinant protein was expressed and purified as described above. The purified MBP-His$_6$-TRX z fusion protein was then subjected to a protease digest using factor Xa (New England Biolabs) to cleave off the maltose binding protein. Cleaved recombinant TRX z was subsequently further purified using nickel-nitrilo-acetic acid agarose (Qiagen). Thioredoxin activity was assessed using the insulin reduction assay as described (Holmgren, 1979). The incubation mixture contained 2 or 5 μM His$_6$-tagged TRX z protein lacking the predicted chloroplast targeting peptide. Recombinant oxidized *E. coli* TRX (Promega) served as a positive control. Fructokinase activity was determined using a coupled optic enzymatic assay as detailed by Karni and Aloni (2002). To investigate the influence of reduction state on enzyme activity, the recombinant proteins were incubated in the pres-

ence of 50 mM DTT, 4 μM recombinant TRX z, or a combination of 10 mM DTT and 4 μM TRX z for 60 min at room temperature prior to the activity measurement. The reaction was started by the addition of 50 mM fructose.

VIGS

VIGS in *N. benthamiana* was performed essentially as described previously (Liu et al., 2002a, 2002b). In brief, fragments of TRX z, FLN1, and FLN2 were amplified by PCR and cloned into pTRV2-Gateway (Liu et al., 2002a) using the Gateway recombination system (Invitrogen). Primer sequences are listed in Supplemental Table 1 online. The resulting plasmids were transformed into *Agrobacterium tumefaciens* C58C1. A lower leaf of a 4-week-old *N. benthamiana* plant (four-leaf stage) was coinfiltrated with a mixture of *Agrobacteria* carrying either pTRV1, a binary vector expressing TRV subgenomic RNA1 under control of the cauliflower mosaic virus 35S promoter, or pTRV2 expressing TRV subgenomic RNA2 and containing the target sequence as described (Liu et al., 2002b). Silenced plants were analyzed 14 d after infiltration.

RNA Extraction and Expression Analysis

Total RNA was isolated from leaf material as described (Logemann et al., 1987) and then treated with RNase-free DNase (Fermentas) to degrade any remaining DNA. First-strand cDNA synthesis was performed from 2 μg of total RNA using a random hexamer using Revert-Aid reverse transcriptase (Fermentas). For RT-PCR, cDNAs were amplified using *Taq* polymerase (New England Biolabs) and gene-specific primers (see Supplemental Table 1 online). The number of amplification cycles was reduced from 35 to 25 to evaluate and quantify any differences among transcript levels before the levels reached saturation. PCR products were separated on a 1% (w/v) agarose gel containing ethidium bromide and visualized by UV light. For quantitative RT-PCR, the cDNAs were amplified using Brilliant II SYBR Green QPCR Mastermix (Stratagene) in an MX3000P real-time PCR instrument (Stratagene). PCR was optimized, and reactions were performed in triplicate. The transcript level was standardized based on cDNA amplification of 18S rRNA as a reference. Relative gene expression data were generated using the wild type in case of *Arabidopsis* or the TRV:GFPsil in case of *N. benthamiana* plants as a calibrator. Fold induction values of target genes were calculated with the $\Delta\Delta$CP equation according to Pfaffl (2001). Statistical analysis was performed using Student's *t* test. Primers used for RT-PCR and quantitative real-time PCR, respectively, are listed in Supplemental Table 1 online.

Yeast Two-Hybrid Assays

Yeast two-hybrid techniques were performed according to the yeast protocols handbook and the Matchmaker GAL4 Two-hybrid System 3 manual (both Clontech) using the yeast reporter strains AH109 and Y187. A fragment of the TRX z coding region comprising amino acids 81 to 183 was amplified by PCR using the primers indicated in Supplemental Table 1 online and inserted via *Eco*RI and *Sal*I into the pGBT-9 vector generating a fusion between the GAL4 DNA binding domain (BD). The yeast strain Y187 carrying the BD-TRX z construct was mated with AH109 cells pretransformed with either a two-hybrid library from *Arabidopsis* inflorescence (Fan et al., 1997; kindly provided by the ABRC) or with a library derived from *Arabidopsis* rosette leaves (Vertis Biotechnology). Diploid cells were selected on medium lacking Leu, Trp, and His supplemented with 4 mM 3-aminotriazole. Cells growing on selective medium were further tested for activity of the *lacZ* reporter gene using filter lift assays. Library plasmids from *his3/lacZ* positive clones were isolated from yeast cells and transformed into *E. coli* before sequencing of the cDNA inserts. Direct interaction of two proteins was investigated by

cotransformation of the respective plasmids in the yeast strain AH109, followed by selection of transformants on medium lacking Leu and Trp at 30°C for 3 d and subsequent transfer to medium lacking Leu, Trp, and His for growth selection and *lacZ* activity testing of interacting clones.

Quantitative LacZ measurements were performed in yeast strain Y190 using *o*-nitrophenyl-β-D-galactopyranoside (ONPG) as a substrate. One unit of β-galactosidase was defined as the amount that hydrolyzes 1 μmol ONPG to *o*-nitrophenol and D-galactose per min per cell.

Protein Extraction, Antibody Generation, and Immunoblotting

Arabidopsis Col-0 wild-type and *trx z* plants from sucrose-supplemented plates were harvested during growth in the light and after 1 h in darkness. Individual pools of one to five plantlets were ground to fine powder under liquid nitrogen. The conditions for the trichloroacetic acid/diethyl ether protein extraction SDS-PAGE are as specified before (Hendriks et al., 2003), and for nonreducing protein electrophoresis, DTT was omitted from the sample buffer. A peptide antibody against FLN2 was produced in rabbit using the peptide C-ITEKEYRTSKPYDE for immunization. The total IgG fraction was purified from the serum and used as primary antibody (dilution 1:1000) in further analyses. Immunoblotting was performed on nitrocellulose membrane (GE Healthcare) according to standard protocols. The signal was detected using the horseradish peroxidase in combination with the ECl plus kit (GE Healthcare) according to the manufacturer's instructions. The polyacrylamide gels were stained using Coomasie Brilliant Blue G 250 and destained in water as previously described (Neuhoff et al., 1988).

Site-Directed Mutagenesis

Site directed mutagenesis of TRX *z* and FLN constructs was performed using the Quick-change site-directed mutagenesis kit (Stratagene) employing primers listed in Supplemental Table 1 online. All base changes were verified by sequencing.

Phylogenetic Analysis

The genomes of *Oryza sativa* ssp *japonica* (at the National Center for Biotechnology Information), *Physcomitrella patens* ssp *patens* v1.1, *Chlamydomonas reinhardtii* (v.3.1), *Acaryochloris marina*, *Anabaena variabilis*, Nostoc sp PCC 7120, and *Synechocystis* sp PCC 6803 (http://genome.jgi-psf.org/) were searched for genes encoding fructokinase-like proteins with similarity to the pfkB carbohydrate kinase family of *Arabidopsis* using the BLASTP algorithm (Altschul et al., 1990). The selected sequences were supplemented with experimentally proven fructokinases from tomato (*Solanum lycopersicum*). The At1g50320 (TRX *x*) protein sequence was used to search the TAIR database (www.Arabidopsis.org) for other members of the thioredoxin family.

The protein sequences were aligned using Muscle v3.7 (Edgar, 2004) using the default settings. Any regions of the gene models that appeared to contain nonconserved insertions or deletions were manually checked for the presence of incorrectly annotated intron/exon splice sites and the gene models corrected if necessary. The corrected protein sequence alignments were manually edited using GeneDoc (Nicholas et al., 1997). The resulting alignments are available as Supplemental Data Sets 1 and 2 online. The phylogenetic analyses were performed using MEGA4 (Tamura et al., 2007). The evolutionary history was inferred using the neighbor-joining method (Saitou and Nei, 1987). The percentage of replicate trees in which the associated taxa clustered together in the bootstrap test (1000 replicates) is shown next to each branch (Felsenstein, 1985). The tree is drawn to scale, with branch lengths representing the evolutionary distance units used to infer the phylogenetic tree. The evolutionary distances were computed using the JTT matrix-based method (Jones et al., 1992) and show the number of amino acid substitutions per site. All positions containing gaps and missing data were eliminated from the data set, and the optimal (bootstrap consensus) trees are shown.

Accession Numbers

If not otherwise stated, sequence data from this article can be found in the Arabidopsis Genome Initiative or GenBank/EMBL databases under the following accession numbers: At3g06730 (At TRX *z*), At1g50320 (At TRX *x*) At3g54090 (At FLN1), At1g69200 (At FLN2), AY323226.1 (Sl FRK3), HM211399 (Nb FLN1), HM211400 (Nb FLN2), CN746716.1 (Nb TRX *f1*), and CN747967.1 (Nb TRX *x*). Accession numbers of proteins used for sequence alignments can be found in the legend to the respective figure.

Author Contributions

B.A., W.L., and F.B. designed research. U.H., M.W., B.A., E.G., S.Ü., M.M., K.P., W.L., and F.B. performed the experiments. U.H., M.W., B.A., W.L., and F.B. analyzed the data. B.A. and F.B. wrote the article.

Supplemental Data

The following materials are available in the online version of the article.

Supplemental Figure 1. Alignment of the Amino Acid Sequences of TRX *z* Proteins.

Supplemental Figure 2. Molecular Analysis of the *trx z Arabidopsis* T-DNA Insertion Mutant Complemented with a CaMV 35S:*TRX z* Expression Construct.

Supplemental Figure 3. FLN1 (At3g54090) and FLN2 (At1g69200) Contain a Conserved Fructokinase Domain.

Supplemental Figure 4. Control Experiments for BiFC Assays.

Supplemental Figure 5. Alignment of the Amino Acid Sequences of FLN1 and FLN2 Proteins.

Supplemental Figure 6. Fructokinase Activity of rRecombinant MBP-FLN1, MBP-FLN2, and MBP-FRK3.

Supplemental Figure 7. Phylogenetic Tree of Selected Members of the pfkB Carbohydrate Kinase Family.

Supplemental Figure 8. Alignment of the Amino Acid Sequences of Experimentally Proven Fructokinases from Plants.

Supplemental Table 1. Primers Used in This Study.

Supplemental Data Set 1. Thioredoxin Protein Alignment Used to Construct the Phylogenetic Tree in Figure 1C.

Supplemental Data Set 2. Alignment of pfkb Carbohydrate Kinase Proteins Used to Generate the Phylogenetic Tree Featured in Supplemental Figure 7.

REFERENCES

Alkhalfioui, F., Renard, M., Vensel, W.H., Wong, J., Tanaka, C.K., Hurkman, W.J., Buchanan, B.B., and Montrichard, F. (2007). Thioredoxin-linked proteins are reduced during germination of *Medicago truncatula* seeds. Plant Physiol. **144:** 1559–1579.

Altschul, S.F., Gish, W., Miller, W., Myers, E.W., and Lipman, D.J. (1990). Basic local alignment search tool. J. Mol. Biol. **215:** 403–410.

Balmer, Y., Koller, A., del Val, G., Manieri, W., Schürmann, P., and Buchanan, B.B. (2003). Proteomics gives insight into the regulatory function of chloroplast thioredoxins. Proc. Natl. Acad. Sci. USA **100:** 370–375.

Balmer, Y., Koller, A., Val, G.D., Schürmann, P., and Buchanan, B.B. (2004a). Proteomics uncovers proteins interacting electrostatically with thioredoxin in chloroplasts. Photosynth. Res. **79:** 275–280.

Balmer, Y., Vensel, W.H., Cai, N., Manieri, W., Schürmann, P., Hurkman, W.J., and Buchanan, B.B. (2006). A complete ferredoxin/thioredoxin system regulates fundamental processes in amyloplasts. Proc. Natl. Acad. Sci. USA **103:** 2988–2993.

Balmer, Y., Vensel, W.H., Tanaka, C.K., Hurkman, W.J., Gelhaye, E., Rouhier, N., Jacquot, J.P., Manieri, W., Schürmann, P., Droux, M., and Buchanan, B.B. (2004b). Thioredoxin links redox to the regulation of fundamental processes of plant mitochondria. Proc. Natl. Acad. Sci. USA **101:** 2642–2647.

Baumgartner, B.J., Rapp, J.C., and Mullet, J.E. (1993). Plastid genes encoding the transcription/translation apparatus are differentially transcribed early in barley (*Hordeum vulgare*) chloroplast development (evidence for selective stabilization of psbA mRNA). Plant Physiol. **101:** 781–791.

Bork, P., Sander, C., and Valencia, A. (1993). Convergent evolution of similar enzymatic function on different protein folds: The hexokinase, ribokinase, and galactokinase families of sugar kinases. Protein Sci. **2:** 31–40.

Börnke, F., Hajirezaei, M., Heineke, D., Melzer, M., Herbers, K., and Sonnewald, U. (2002). High-level production of the non-cariogenic sucrose isomer palatinose in transgenic tobacco plants strongly impairs development. Planta **214:** 356–364.

Brigneti, G., Voinnet, O., Li, W.X., Ji, L.H., Ding, S.W., and Baulcombe, D.C. (1998). Viral pathogenicity determinants are suppressors of transgene silencing in *Nicotiana benthamiana*. EMBO J. **17:** 6739–6746.

Brodegger, T., Stockmann, A., Oberstrass, J., Nellen, W., and Follmann, H. (2004). Novel thioredoxin targets in *Dictyostelium discoideum* identified by two-hybrid analysis: Interactions of thioredoxin with elongation factor 1 alpha and yeast alcohol dehydrogenase. Biol. Chem. **385:** 1185–1192.

Buchanan, B.B. (1980). Role of light in the regulation of chloroplast enzymes. Annu. Rev. Plant Physiol. **31:** 341–374.

Buchanan, B.B., and Balmer, Y. (2005). Redox regulation: A broadening horizon. Annu. Rev. Plant Biol. **56:** 187–220.

Caplan, J.L., Mamillapalli, P., Burch-Smith, T.M., Czymmek, K., and Dinesh-Kumar, S.P. (2008). Chloroplastic protein NRIP1 mediates innate immune receptor recognition of a viral effector. Cell **132:** 449–462.

Chen, S., Hofius, D., Sonnewald, U., and Börnke, F. (2003). Temporal and spatial control of gene silencing in transgenic plants by inducible expression of double-stranded RNA. Plant J. **36:** 731–740.

Chi, Y.H., et al. (2008). Abnormal chloroplast development and growth inhibition in rice thioredoxin m knock-down plants. Plant Physiol. **148:** 808–817.

Clough, S.J., and Bent, A.F. (1998). Floral dip: A simplified method for *Agrobacterium*-mediated transformation of *Arabidopsis thaliana.* Plant J. **16:** 735–743.

Collin, V., Issakidis-Bourguet, E., Marchand, C., Hirasawa, M., Lancelin, J.M., Knaff, D.B., and Miginiac-Maslow, M. (2003). The *Arabidopsis* plastidial thioredoxins: new functions and new insights into specificity. J. Biol. Chem. **278:** 23747–23752.

Collin, V., Lamkemeyer, P., Miginiac-Maslow, M., Hirasawa, M., Knaff, D.B., Dietz, K.J., and Issakidis-Bourguet, E. (2004). Characterization of plastidial thioredoxins from Arabidopsis belonging to the new y-type. Plant Physiol. **136:** 4088–4095.

Damari-Weissler, H., Kandel-Kfir, M., Gidoni, D., Mett, A., Belausov, E., and Granot, D. (2006). Evidence for intracellular spatial separation of hexokinases and fructokinases in tomato plants. Planta **224:** 1495–1502.

Durek, P., Schmidt, R., Heazlewood, J.L., Jones, A., MacLean, D., Nagel, A., Kersten, B., and Schulze, W.X. (2010). PhosPhAt: The *Arabidopsis thaliana* phosphorylation site database. An update. Nucleic Acids Res. **38:** D828–D834.

Edgar, R.C. (2004). MUSCLE: Multiple sequence alignment with high accuracy and high throughput. Nucleic Acids Res. **32:** 1792–1797.

Emanuelsson, O., Nielsen, H., and von Heijne, G. (1999). ChloroP, a neural network-based method for predicting chloroplast transit peptides and their cleavage sites. Protein Sci. **8:** 978–984.

Fan, H.Y., Hu, Y., Tudor, M., and Ma, H. (1997). Specific interactions between the K domains of AG and AGLs, members of the MADS domain family of DNA binding proteins. Plant J. **12:** 999–1010.

Felsenstein, J. (1985). Confidence limits on phylogenies - An approach using the bootstrap. Evolution **39:** 783–791.

Garcia, M., Myouga, F., Takechi, K., Sato, H., Nabeshima, K., Nagata, N., Takio, S., Shinozaki, K., and Takano, H. (2008). An Arabidopsis homolog of the bacterial peptidoglycan synthesis enzyme MurE has an essential role in chloroplast development. Plant J. **53:** 924–934.

Gelhaye, E., Rouhier, N., Navrot, N., and Jacquot, J.P. (2005). The plant thioredoxin system. Cell. Mol. Life Sci. **62:** 24–35.

Gelhaye, E., et al. (2004). A specific form of thioredoxin h occurs in plant mitochondria and regulates the alternative oxidase. Proc. Natl. Acad. Sci. USA **101:** 14545–14550.

German, M.A., Asher, I., Petreikov, M., Dai, N., Schaffer, A.A., and Granot, D. (2004). Cloning, expression and characterization of LeFRK3, the fourth tomato (*Lycopersicon esculentum* Mill.) gene encoding fructokinase. Plant Sci. **166:** 285–291.

Hajdukiewicz, P.T., Allison, L.A., and Maliga, P. (1997). The two RNA polymerases encoded by the nuclear and the plastid compartments transcribe distinct groups of genes in tobacco plastids. EMBO J. **16:** 4041–4048.

Hanaoka, M., Kanamaru, K., Fujiwara, M., Takahashi, H., and Tanaka, K. (2005). Glutamyl-tRNA mediates a switch in RNA polymerase use during chloroplast biogenesis. EMBO Rep. **6:** 545–550.

Hendriks, J.H.M., Kolbe, A., Gibon, Y., Stitt, M., and Geigenberger, P. (2003). ADP-glucose pyrophosphorylase is activated by posttranslational redox-modification in response to light and to sugars in leaves of Arabidopsis and other plant species. Plant Physiol. **133:** 838–849.

Holmgren, A. (1979). Thioredoxin catalyzes the reduction of insulin disulfides by dithiothreitol and dihydrolipoamide. J. Biol. Chem. **254:** 9627–9632.

Issakidis-Bourguet, E., Mouaheb, N., Meyer, Y., and Miginiac-Maslow, M. (2001). Heterologous complementation of yeast reveals a new putative function for chloroplast m-type thioredoxin. Plant J. **25:** 127–135.

Jones, D.T., Taylor, W.R., and Thornton, J.M. (1992). The rapid generation of mutation data matrices from protein sequences. Comput. Appl. Biosci. **8:** 275–282.

Karimi, M., Inzé, D., and Depicker, A. (2002). GATEWAY(TM) vectors for *Agrobacterium*-mediated plant transformation. Trends Plant Sci. **7:** 193–195.

Karni, L., and Aloni, B. (2002). Fructokinase and hexokinase from pollen grains of bell pepper (*Capsicum annuum* L.): Possible role in pollen germination under conditions of high temperature and CO_2 enrichment. Ann. Bot. (Lond.) **90:** 607–612.

Kettunen, R., Pursiheimo, S., Rintamäki, E., VanWijk, K.J., and Aro, E.M. (1997). Transcriptional and translational adjustments of *psbA* gene expression in mature chloroplasts during photoinhibition and subsequent repair of photosystem II. Eur. J. Biochem. **247:** 441–448.

Koussevitzky, S., Nott, A., Mockler, T.C., Hong, F., Sachetto-Martins, G., Surpin, M., Lim, J., Mittler, R., and Chory, J. (2007). Signals from chloroplasts converge to regulate nuclear gene expression. Science **316:** 715–719.

Laloi, C., Rayapuram, N., Chartier, Y., Grienenberger, J.M., Bonnard, G., and Meyer, Y. (2001). Identification and characterization of a mitochondrial thioredoxin system in plants. Proc. Natl. Acad. Sci. USA **98:** 14144–14149.

Lepistö, A., Kangasjärvi, S., Luomala, E.-M., Brader, G., Sipari, N., Keränen, M., Keinänen, M., and Rintamäki, E. (2009). Chloroplast NADPH-thioredoxin reductase interacts with photoperiodic development in Arabidopsis. Plant Physiol. **149:** 1261–1276.

Li, K., Pasternak, C., Hartig, E., Haberzettl, K., Maxwell, A., and Klug, G. (2004). Thioredoxin can influence gene expression by affecting gyrase activity. Nucleic Acids Res. **32:** 4563–4575.

Liu, Y., Schiff, M., and Dinesh-Kumar, S.P. (2002a). Virus-induced gene silencing in tomato. Plant J. **31:** 777–786.

Liu, Y., Schiff, M., Marathe, R., and Dinesh-Kumar, S.P. (2002b). Tobacco Rar1, EDS1 and NPR1/NIM1 like genes are required for N-mediated resistance to tobacco mosaic virus. Plant J. **30:** 415–429.

Logemann, J., Schell, J., and Willmitzer, L. (1987). Improved method for the isolation of RNA from plant tissues. Anal. Biochem. **163:** 16–20.

Marchand, C., Le Marechal, P., Meyer, Y., and Decottignies, P. (2006). Comparative proteomic approaches for the isolation of proteins interacting with thioredoxin. Proteomics **6:** 6528–6537.

Marchler-Bauer, A., et al. (2009). CDD: Specific functional annotation with the Conserved Domain Database. Nucleic Acids Res. **37:** D205–D210.

Meyer, Y., Reichheld, J.P., and Vignols, F. (2005). Thioredoxins in Arabidopsis and other plants. Photosynth. Res. **86:** 419–433.

Meyer, Y., Siala, W., Bashandy, T., Riondet, C., Vignols, F., and Reichheld, J.P. (2008). Glutaredoxins and thioredoxins in plants. Biochim. Biophys. Acta **1783:** 589–600.

Miallau, L., Hunter, W.N., McSweeney, S.M., and Leonard, G.A. (2007). Structures of *Staphylococcus aureus* D-tagatose-6-phosphate kinase implicate domain motions in specificity and mechanism. J. Biol. Chem. **282:** 19948–19957.

Michalska, J., Zauber, H., Buchanan, B.B., Cejudo, F.J., and Geigenberger, P. (2009). NTRC links built-in thioredoxin to light and sucrose in regulating starch synthesis in chloroplasts and amyloplasts. Proc. Natl. Acad. Sci. USA **106:** 9908–9913.

Mochizuki, N., Brusslan, J.A., Larkin, R., Nagatani, A., and Chory, J. (2001). Arabidopsis genomes uncoupled 5 (GUN5) mutant reveals the involvement of Mg-chelatase H subunit in plastid-to-nucleus signal transduction. Proc. Natl. Acad. Sci. USA **98:** 2053–2058.

Motohashi, K., Kondoh, A., Stumpp, M.T., and Hisabori, T. (2001). Comprehensive survey of proteins targeted by chloroplast thioredoxin. Proc. Natl. Acad. Sci. USA **98:** 11224–11229.

Nekrasov, V., Ludwig, A.A., and Jones, J.D. (2006). CITRX thioredoxin is a putative adaptor protein connecting Cf-9 and the ACIK1 protein kinase during the Cf-9/Avr9- induced defence response. FEBS Lett. **580:** 4236–4241.

Nicholas, K.B., Nicholas, H.B., Jr., Deerfield II, D.W. (1997). GeneDoc: Analysis and visualization of genetic variation. EMBnet.news **4:** 1–4.

Nishiyama, A., Matsui, M., Iwata, S., Hirota, K., Masutani, H.,

Nakamura, H., Takagi, Y., Sono, H., Gon, Y., and Yodoi, J. (1999). Identification of Thioredoxin-binding Protein-2/Vitamin D3 Up-regulated Protein 1 as a negative regulator of thioredoxin function and expression. J. Biol. Chem. **274:** 21645–21650.

Nott, A., Jung, H.S., Koussevitzky, S., and Chory, J. (2006). Plastid-to-nucleus retrograde signaling. Annu. Rev. Plant Biol. **57:** 739–759.

Neuhoff, V., Arold, N., Taube, D., and Ehrhardt, W. (1988). Improved staining of proteins in polyacrylamide gels including isoelectric focusing gels with clear background at nanogram sensitivity using Coomassie Brilliant Blue G-250 and R-250. Electrophoresis **9:** 255–262.

Pasternak, C., Haberzettl, K., and Klug, G. (1999). Thioredoxin is involved in oxygen-regulated formation of the photosynthetic apparatus of *Rhodobacter sphaeroides.* J. Bacteriol. **181:** 100–106.

Pfaffl, M.W. (2001). A new mathematical model for relative quantification in real-time RT-PCR. Nucleic Acids Res. **29:** e45.

Pfalz, J., Liere, K., Kandlbinder, A., Dietz, K.J., and Oelmuller, R. (2006). pTAC2, -6, and -12 are components of the transcriptionally active plastid chromosome that are required for plastid gene expression. Plant Cell **18:** 176–197.

Pfannschmidt, T., and Liere, K. (2005). Redox regulation and modification of proteins controlling chloroplast gene expression. Antioxid. Redox Signal. **7:** 607–618.

Pfannschmidt, T., Nilsson, A., and Allen, J.F. (1999). Photosynthetic control of chloroplast gene expression. Nature **397:** 625–628.

Pogson, B.J., Woo, N.S., Förster, B., and Small, I.D. (2008). Plastid signalling to the nucleus and beyond. Trends Plant Sci. **13:** 602–609.

Puthiyaveetil, S., Kavanagh, T.A., Cain, P., Sullivan, J.A., Newell, C.A., Gray, J.C., Robinson, C., van der Giezen, M., Rogers, M.B., and Allen, J.F. (2008). The ancestral symbiont sensor kinase CSK links photosynthesis with gene expression in chloroplasts. Proc. Natl. Acad. Sci. USA **105:** 10061–10066.

Rivas, S., Rougon-Cardoso, A., Smoker, M., Schauser, L., Yoshioka, H., and Jones, J.D. (2004). CITRX thioredoxin interacts with the tomato Cf-9 resistance protein and negatively regulates defence. EMBO J. **23:** 2156–2165.

Ronimus, R.S., and Morgan, H.W. (2001). The biochemical properties and phylogenies of phosphofructokinases from extremophiles. Extremophiles **5:** 357–373.

Saitou, N., and Nei, M. (1987). The neighbor-joining method: A new method for reconstructing phylogenetic trees. Mol. Biol. Evol. **4:** 406–425.

Sato, N., Albrieux, C., Joyard, J., Douce, R., and Kuroiwa, T. (1993). Detection and characterization of a plastid envelope DNA-binding protein which may anchor plastid nucleoids. EMBO J. **12:** 555–561.

Schmid, M., Davison, T.S., Henz, S.R., Pape, U.J., Demar, M., Vingron, M., Scholkopf, B., Weigel, D., and Lohmann, J.U. (2005). A gene expression map of *Arabidopsis thaliana* development. Nat. Genet. **37:** 501–506.

Schulze-Osthoff, K., Schenk, H., and Droge, W. (1995). Effects of thioredoxin on activation of transcription factor NF-kappa B. Methods Enzymol. **252:** 253–264.

Schürmann, P., and Jacquot, J.P. (2000). Plant thioredoxin systems revisited. Annu. Rev. Plant Physiol. Plant Mol. Biol. **51:** 371–400.

Sekine, K., Fujiwara, M., Nakayama, M., Takao, T., Hase, T., and Sato, N. (2007). DNA binding and partial nucleoid localization of the chloroplast stromal enzyme ferredoxin:sulfite reductase. FEBS J. **274:** 2054–2069.

Sekine, K., Hase, T., and Sato, N. (2002). Reversible DNA compaction by sulfite reductase regulates transcriptional activity of chloroplast nucleoids. J. Biol. Chem. **277:** 24399–24404.

Serrato, A.J., Perez-Ruiz, J.M., Spinola, M.C., and Cejudo, F.J. (2004). A novel NADPH thioredoxin reductase, localized in the

chloroplast, which deficiency causes hypersensitivity to abiotic stress in *Arabidopsis thaliana*. J. Biol. Chem. **279:** 43821–43827.

Shiina, T., Allison, L., and Maliga, P. (1998). *rbcL* transcript levels in tobacco plastids are independent of light: Reduced dark transcription rate is compensated by increased mRNA stability. Plant Cell **10:** 1713–1722.

Shiina, T., Tsunoyama, Y., Nakahira, Y., and Khan, M.S. (2005). Plastid RNA polymerases, promoters, and transcription regulators in higher plants. Int. Rev. Cytol. **244:** 1–68.

Sigrell, J.A., Cameron, A.D., Jones, T.A., and Mowbray, S.L. (1998). Structure of *Escherichia coli* ribokinase in complex with ribose and dinucleotide determined to 1.8 A resolution: insights into a new family of kinase structures. Structure **6:** 183–193.

Spinola, M.C., Perez-Ruiz, J.M., Pulido, P., Kirchsteiger, K., Guinea, M., Gonzalez, M., and Cejudo, F.J. (2008). NTRC new ways of using NADPH in the chloroplast. Physiol. Plant. **133:** 516–524.

Steiner, S., Dietzel, L., Schröter, Y., Fey, V., Wagner, R., and Pfannschmidt, T. (2009). The role of phosphorylation in redox regulation of photosynthesis genes *psaA* and *psbA* during photosynthetic acclimation of mustard. Mol. Plant **2:** 416–429.

Steinhauser, D., Usadel, B., Luedemann, A., Thimm, O., and Kopka, J. (2004). CSB.DB: A comprehensive systems-biology database. Bioinformatics **20:** 3647–3651.

Susek, R.E., Ausubel, F.M., and Chory, J. (1993). Signal transduction mutants of *Arabidopsis* uncouple nuclear CAB and RBCS gene expression from chloroplast development. Cell **74:** 787–799.

Suzuki, J.Y., Jimmy Ytterberg, A., Beardslee, T.A., Allison, L.A., Wijk, K.J., and Maliga, P. (2004). Affinity purification of the tobacco

plastid RNA polymerase and in vitro reconstitution of the holoenzyme. Plant J. **40:** 164–172.

Tamura, K., Dudley, J., Nei, M., and Kumar, S. (2007). MEGA4: Molecular Evolutionary Genetics Analysis (MEGA) software version 4.0. Mol. Biol. Evol. **24:** 1596–1599.

Verdoucq, L., Vignols, F., Jacquot, J.P., Chartier, Y., and Meyer, Y. (1999). In vivo characterization of a thioredoxin h target protein defines a new peroxiredoxin family. J. Biol. Chem. **274:** 19714–19722.

Vignols, F., Brehelin, C., Surdin-Kerjan, Y., Thomas, D., and Meyer, Y. (2005). A yeast two-hybrid knockout strain to explore thioredoxin-interacting proteins in vivo. Proc. Natl. Acad. Sci. USA **102:** 16729–16734.

Wachter, A., Wolf, S., Steininger, H., Bogs, J., and Rausch, T. (2005). Differential targeting of GSH1 and GSH2 is achieved by multiple transcription initiation: Implications for the compartmentation of glutathione biosynthesis in the *Brassicaceae*. Plant J. **41:** 15–30.

Walter, M., Chaban, C., Schutze, K., Batistic, O., Weckermann, K., Nake, C., Blazevic, D., Grefen, C., Schumacher, K., Oecking, C., Harter, K., and Kudla, J. (2004). Visualization of protein interactions in living plant cells using bimolecular fluorescence complementation. Plant J. **40:** 428–438.

Wong, J.H., Cai, N., Balmer, Y., Tanaka, C.K., Vensel, W.H., Hurkman, W.J., and Buchanan, B.B. (2004). Thioredoxin targets of developing wheat seeds identified by complementary proteomic approaches. Phytochemistry **65:** 1629–1640.

Yamanaka, H., Maehira, F., Oshiro, M., Asato, T., Yanagawa, Y., Takei, H., and Nakashima, Y. (2000). A possible interaction of thioredoxin with VDUP1 in HeLa cells detected in a yeast two-hybrid system. Biochem. Biophys. Res. Commun. **271:** 796–800.